



Spatial Generalized Linear Models in R Using **spmodel**

Michael Dumelle 

United States
Environmental Protection Agency

Jay M. Ver Hoef 

Alaska Fisheries
Science Center

Matt Higham 

St. Lawrence University

Abstract

Non-Gaussian data are common in practice and include binary, count, skewed, and proportion data types. Often, non-Gaussian data are modeled using a generalized linear model (GLM). GLMs typically assume that observations are independent of one another. This is an impractical assumption for spatial data, as nearby observations tend to be more similar than distant ones. The **spmodel** package in R provides a suite of tools for fitting spatial generalized linear models (SPGLMs) to non-Gaussian data and making spatial predictions (i.e., Kriging). SPGLMs for point-referenced data (x- and y-coordinates) are fit using the `spglm()` function, while SPGLMs for areal (lattice, polygon) data are fit using the `spgautor()` function. Both `spglm()` and `spgautor()` maximize a novel Laplace likelihood which marginalizes over the model's fixed effects and latent mean while formally incorporating spatial covariance (i.e., spatial correlation). The inputs and outputs of `spglm()` and `spgautor()` closely resemble the `glm()` function from base R, easing the transition from GLMs to SPGLMs. **spmodel** provides and builds upon several commonly used helper functions for model building like `summary()`, `plot()`, `fitted()`, and `tidy()`, among others. Spatial predictions of the latent mean at unobserved locations are obtained using `predict()` or `augment()`. **spmodel** accommodates myriad advanced modeling features like geometric anisotropy, nonspatial random effects, analysis of variance, and more. Throughout, we use **spmodel** to fit SPGLMs to moose presence and counts in Alaska, United States (US), skewed conductivity data in the Southwestern US, harbor seal abundance trends in Alaska, US, and voter turnout rates in Texas, US.

Keywords: autoregressive model, geostatistical model, spatial covariance, spatial correlation.

1. Introduction

1 In practice, non-Gaussian data (e.g., binary, count, skewed, and proportion data) are ubiq-
 2 uitous. Non-Gaussian data that belong to an exponential family can be naturally modeled
 3 using a generalized linear model (GLM) regression framework (Nelder and Wedderburn 1972;
 4 McCullagh and Nelder 1989). In a GLM, an $n \times 1$ response variable \mathbf{y} belongs to a statistical
 5 distribution (e.g., Binomial, Poisson) with some mean and variance. Often, the analysis goal
 6 is to study the impact of a linear function of several explanatory variables on \mathbf{y} through a
 7 GLM. In this context, the latent (i.e., unobserved) mean of \mathbf{y} , $\boldsymbol{\mu}$, is linked to these explanatory
 8 variables via a link function:

$$f(\boldsymbol{\mu}|\mathbf{X}, \boldsymbol{\beta}) \equiv \mathbf{w} = \mathbf{X}\boldsymbol{\beta}, \quad (1)$$

9 where for a sample size n , $f(\cdot)$ is a link function that connects $\boldsymbol{\mu}$ to \mathbf{w} , \mathbf{X} is the $n \times p$
 10 design matrix of explanatory variables, and $\boldsymbol{\beta}$ is the $p \times 1$ vector of fixed effects. While the
 11 mean is typically constrained in some way (e.g., if a probability, between zero and one), the
 12 link function generally makes \mathbf{w} unconstrained. Common link functions include the log odds
 13 (i.e., logit) link for binary and proportion data and the log link for count and skewed data.
 14 Equation 1 can also be written in terms of the inverse link function, $f^{-1}(\cdot)$:

$$\boldsymbol{\mu}|\mathbf{X}, \boldsymbol{\beta} \equiv f^{-1}(\mathbf{w}) = f^{-1}(\mathbf{X}\boldsymbol{\beta}).$$

15 The GLM fixed effects ($\boldsymbol{\beta}$) are typically estimated via maximum likelihood (Chambers and
 16 Hastie 1992). It is often convenient to compute the maximum likelihood estimates using the
 17 iteratively reweighted least squares (IRWLS) algorithm (Wood 2017), which is the approach
 18 used by the `glm()` function in the R programming language (R Core Team 2024). GLMs
 19 add an additional layer of complexity compared to linear regression models, as the left-hand
 20 side of Equation 1 is a function of the mean of \mathbf{y} rather than \mathbf{y} itself (as in linear regression
 21 models).

22 The standard GLM assumes the elements of \mathbf{y} are independent. This independence assumption
 23 is typically impractical for spatial data. For spatial data, nearby observations tend to be
 24 more similar than distant observations (Tobler 1970), which leads to positive spatial covariance.
 25 The consequences of ignoring spatial covariance in statistical models for spatial data
 26 can be severe and include imprecise parameter estimates as well as misleading standard errors
 27 that inflate Type-I error rates and decrease power (Zimmerman and Ver Hoef 2024).

28 An approach for handling spatial data using a GLM is to assume the elements of \mathbf{w} share
 29 covariance that varies spatially. This is achieved by adding to Equation 1 two random effects,
 30 $\boldsymbol{\tau}$ and $\boldsymbol{\epsilon}$. The random effect $\boldsymbol{\tau}$ is an $n \times 1$ column vector of spatially dependent random errors.
 31 We assume that $E(\boldsymbol{\tau}) = \mathbf{0}$ and $Cov(\boldsymbol{\tau}) = \sigma_{\tau}^2 \mathbf{R}$, where $E(\cdot)$ and $Cov(\cdot)$ denote expectation
 32 and covariance, respectively. The variance parameter σ_{τ}^2 controls the magnitude of spatial
 33 covariance and is often called a partial sill. The matrix \mathbf{R} is an $n \times n$ spatial correlation
 34 matrix that depends on a range parameter controlling the distance-decay rate of the spatial
 35 correlation. One example of a spatial covariance matrix is the “exponential,” which is given
 36 by

$$Cov(\boldsymbol{\tau}) = \sigma_{\tau}^2 \mathbf{R}_{exp} = \sigma_{\tau}^2 \exp(-\mathbf{H}/\phi), \quad (2)$$

37 where \mathbf{H} is a matrix of pairwise distances among the elements of \mathbf{y} and ϕ is the range
 38 parameter. From Equation 2, as the distance between two elements of \mathbf{y} increases, the spatial

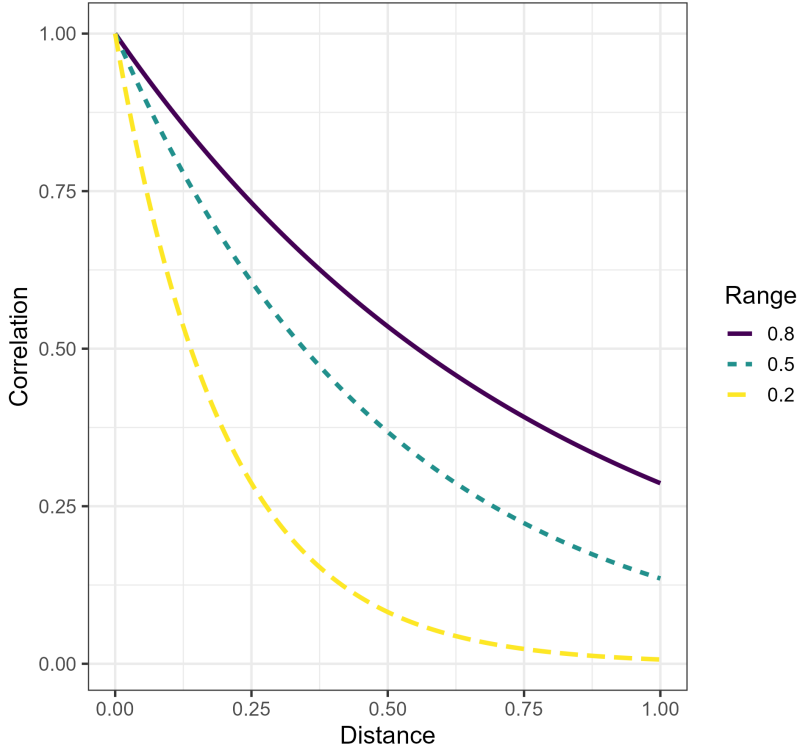


Figure 1: An exponential spatial correlation function with varying range parameters.

39 covariance decreases, which reflects intuition. Moreover, as the range parameter, ϕ , increases,
 40 the strength of spatial dependence increases (Figure 1). The random effect ϵ is an $n \times 1$
 41 column vector of independent random errors. We assume that $E(\epsilon) = \mathbf{0}$ and $\text{Cov}(\tau) = \sigma_\epsilon^2 \mathbf{I}$,
 42 where \mathbf{I} is an $n \times n$ identity matrix. The variance parameter σ_ϵ^2 controls the magnitude
 43 of nonspatial variability (i.e., fine-scale variation) and is often called a nugget. Often in
 44 spatial statistics, quantities are explicitly referenced with respect to \mathbf{s} , a vector of coordinates
 45 indexing the observation (Cressie 1993). For example, \mathbf{y} and \mathbf{X} may instead be written $\mathbf{y}(\mathbf{s})$
 46 and $\mathbf{X}(\mathbf{s})$, respectively. We acknowledge the utility of this nomenclature but drop the explicit
 47 dependence on \mathbf{s} for simplicity of notation.

48 Through inclusion of τ and ϵ , the spatial GLM (SPGLM) can be written as

$$f(\boldsymbol{\mu}|\mathbf{X}, \boldsymbol{\beta}, \boldsymbol{\tau}, \boldsymbol{\epsilon}) \equiv \mathbf{w} = \mathbf{X}\boldsymbol{\beta} + \boldsymbol{\tau} + \boldsymbol{\epsilon}. \quad (3)$$

49 Assuming independence among $\boldsymbol{\tau}$ and $\boldsymbol{\epsilon}$, it follows that

$$\text{Cov}(\boldsymbol{\tau} + \boldsymbol{\epsilon}) = \text{Cov}(\boldsymbol{\tau}) + \text{Cov}(\boldsymbol{\epsilon}) = \sigma_\tau^2 \mathbf{R} + \sigma_\epsilon^2 \mathbf{I}.$$

50 Henceforth, we refer to σ_τ^2 as σ_{de}^2 (for spatially dependent error variance) and σ_ϵ^2 as σ_{ie}^2
 51 (for independent error variance). The parameters σ_{de}^2 , σ_{ie}^2 , and ϕ , in addition to any other
 52 parameters in \mathbf{R} , compose $\boldsymbol{\theta}$, the covariance parameter vector.

53 Fitting and using SPGLMs is challenging both conceptually and computationally (Bolker,
 54 Brooks, Clark, Geange, Poulsen, Stevens, and White 2009). Recently, however, there have
 55 been numerous, significant advances in R software that have made these models more acces-
 56 sible to practitioners. The **brms** (Bürkner 2017), **carBayes** (Lee 2013), **ngspatial** (Hughes and

57 Cui 2020), **R-INLA** (Lindgren and Rue 2015) and **inlabru** (Bachl, Lindgren, Borchers, and
 58 Illian 2019), **spBayes** (Finley, Banerjee, and Carlin 2007), **spOccupancy** (Doser, Finley, Kéry,
 59 and Zipkin 2022), **spAbundance** (Doser, Finley, Kéry, and Zipkin 2024), and **spNNGP** (Finley,
 60 Datta, and Banerjee 2022) packages take a Bayesian approach, either directly sampling from
 61 posterior distributions of parameters (e.g., using MCMC) or approximating them. A benefit
 62 of Bayesian approaches is that prior information can be incorporated and uncertainty quan-
 63 tification of parameter estimates is straightforward. However, Bayesian approaches, especially
 64 those using MCMC, can be computationally expensive. In order to reduce computation time,
 65 many of these packages work with the precision matrix instead of the covariance matrix so
 66 that computationally expensive matrix inversion is not required. For example, **R-INLA** uses
 67 the precision matrix and tends to be very fast. Working with precision matrices, however,
 68 can be more restrictive and less intuitive than working directly with the covariance matrix.
 69 The **FRK** (Sainsbury-Dale, Zammit-Mangion, and Cressie 2024), **glmmTMB** (Brooks, Kris-
 70 tensen, van Benthem, Magnusson, Berg, Nielsen, Skaug, Maechler, and Bolker 2017), **hglm**
 71 (Ronnegard, Shen, and Alam 2010), **mgev** (Wood 2017), and **spaMM** (Rousset and Ferdy
 72 2014) packages directly use Laplace, quasi-likelihood, or reduced-rank approaches to estimate
 73 parameters. These direct approaches tend to be computationally efficient, as they don't rely
 74 on MCMC sampling. In contrast to the Bayesian approach, a drawback of these direct ap-
 75 proaches is that prior information cannot be formally incorporated and covariance parameter
 76 uncertainty is more challenging to quantify. The **sdmTMB** (Anderson, Ward, English, Bar-
 77 nett, and Thorson 2024) package combines elements of **R-INLA**, **glmmTMB**, and Gaussian
 78 Markov random fields to fit a wide variety of SPGLMs, while **tinyVAST** (Thorson, Ander-
 79 son, Goddard, and Rooper 2025) extends some of these models to multivariate or (dynamic)
 80 structural equation models.
 81 Building from Evangelou, Zhu, and Smith (2011) and Bonat and Ribeiro Jr (2016), Ver Hoef,
 82 Blagg, Dumelle, Dixon, Zimmerman, and Conn (2024) proposed a novel approach for fitting
 83 SPGLMs that leverages the Laplace approximation while marginalizing over both the latent
 84 \mathbf{w} and the fixed effects (β) and accommodating spatial covariance. This approach performed
 85 efficiently in a variety of simulation settings, generally having appropriate confidence interval
 86 coverage for the fixed effects and prediction interval coverage for \mathbf{w} at new locations. The
 87 approach performed similarly to the Bayesian SPGLM approach in **spBayes** and the automatic
 88 differentiation SPGLM approach in **glmmTMB** but was much faster. At small sample sizes,
 89 the approach outperformed the approximate Bayesian SPGLM approach in **R-INLA** and had
 90 similar computational times. For moderate sample sizes, it performed similarly to **R-INLA**,
 91 though **R-INLA** was faster. The novel Laplace approach is particularly attractive for two
 92 reasons. First, it is general enough that it can be applied to any covariance structure (not
 93 just spatial). Second, after estimating the covariance parameters, analytical solutions exist
 94 for the fixed effects (and their standard errors) as well as predictions of the latent \mathbf{w} at new
 95 locations (and their standard errors).
 96 The **spmodel** R package (Dumelle, Higham, and Ver Hoef 2023) recently provided a full set
 97 of modeling tools for SPGLMs fit using the novel Laplace approach described by Ver Hoef
 98 *et al.* (2024). These modeling tools are approachable and mirror the familiar **glm()** syntax
 99 from base-R, making the transition from GLMs to SPGLMs relatively seamless. The **spglm()**
 100 function fits SPGLMs for point-referenced data (e.g., x-coordinates and y-coordinates repre-
 101 senting point locations in a field; models are sometimes called “geostatistical” models), while
 102 the **spgautor()** function fits SPGLMs for areal data (e.g., polygon boundaries representing

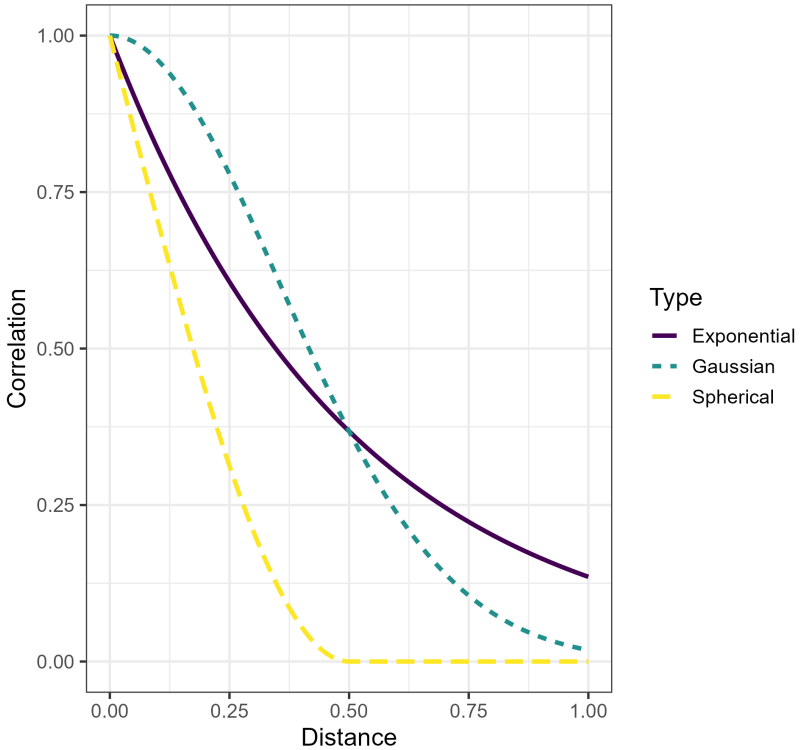


Figure 2: Exponential, Gaussian, and spherical spatial correlation functions all with range parameters equal to 0.5.

103 geographic subsets of a region; models are sometimes called “autoregressive” models). For
 104 both point-referenced data and areal data, **spmodel** supports the binomial distribution for
 105 binary data, Poisson and negative binomial distributions for count data, Gamma and inverse
 106 Gaussian distributions for skewed data, and the beta distribution for proportion data. There
 107 are 20 different spatial covariance structures available including the exponential, Gaussian,
 108 and spherical for point-referenced data (Figure 2) and the conditional autoregressive, and
 109 simultaneous autoregressive structures for areal data. **spmodel** provides tools for commonly
 110 used model summaries, visualizations, and diagnostics (e.g., Cook’s distance) using standard
 111 R helper functions like `summary()`, `plot()`, `fitted()`, and `tidy()`, among others. **spmodel**
 112 also provides tools to predict `w` at new locations and quantify uncertainty in those prediction
 113 using `predict()` and `augment()`. This core functionality, combined with several advanced
 114 features we describe throughout the manuscript, enables **spmodel** to introduce novel, impor-
 115 tant SPGLM modeling tools previously missing from the existing R ecosystem.
 116 Of the existing R packages for SPGLMs, **spmodel** (version 0.11.0) is arguably most similar
 117 to **sdmTMB** (version 0.7.4) in terms of scope and feel. Both packages use similar syntax
 118 as `glm()`, accommodate flexible `formula` arguments (e.g., offsets, splines), handle spatial
 119 covariance that decays at different rates in different directions (i.e., geometric anisotropy),
 120 incorporate nonspatial random effects, support other R packages for modeling like **broom**
 121 (Robinson, Hayes, and Couch 2021; Kuhn and Silge 2022), **emmeans** (Lenth 2024), and **car**
 122 (Fox and Weisberg 2019), and have tools for model summaries, prediction, and simulating
 123 data. There are some notable differences between the two packages, however. **sdmTMB** sup-

¹²⁴ ports several additional GLM distributions like the Tweedie, supports Hurdle models, and can
¹²⁵ incorporate prior information through Bayesian applications. **sdmTMB** also provides tools for
¹²⁶ working with temporal data and spatiotemporal data and provides enhanced visualizations
¹²⁷ of the model's marginal effects. **sdmTMB** does require a preprocessing step of constructing
¹²⁸ a mesh for the stochastic partial differential equation approach, and the density of the mesh
¹²⁹ can affect model results and computational complexity. On the other hand, **spmodel** does
¹³⁰ not require the construction of a mesh prior to modeling. **spmodel** also supports 20 different
¹³¹ spatial covariances and models them directly, rather than using a precision matrix approx-
¹³² imation to the Matérn spatial covariance as in **sdmTMB**. **spmodel** can model data directly
¹³³ using neighborhood distance and autoregressive models, rather than relying on the polygon
¹³⁴ centroid (as in **sdmTMB**), which may not be within the polygon's boundaries. **spmodel** pro-
¹³⁵ vides experimental design tools (e.g., analysis of variance, contrasts), supports **sf** objects in
¹³⁶ modeling and prediction functions (Pebesma 2018), has several specialized model diagno-
¹³⁷ stics like leverage values and Cook's distances, and has analytic solutions for fixed effect and
¹³⁸ prediction standard errors. Other similarities and differences do exist between **sdmTMB** and
¹³⁹ **spmodel**, and both packages continue to evolve. Overall, we believe that these packages are
¹⁴⁰ complementary and enhance the suite of SPGLM tools accessible to practitioners.

¹⁴¹ The rest of this article is organized as follows. In Section 2, we provide some background for
¹⁴² the SPGLM fitting and prediction routines in **spmodel**. In Section 3, we provide an overview
¹⁴³ of core SPGLM functionality in **spmodel** by modeling moose presence in Alaska, United
¹⁴⁴ States (US). In Section 4, we model moose counts in Alaska, US; skewed lake conductivity
¹⁴⁵ in the Southwestern US; harbor seal abundance trend behavior in Alaska, US; and voter
¹⁴⁶ turnout rates in Texas, US. And in Section 5, we end with a discussion synthesizing **spmodel**'s
¹⁴⁷ contributions to the analysis of SPGLMs in R.

2. The spatial generalized linear model and marginalization

¹⁴⁸ The novel Laplace approach implemented in **spmodel** formally maximizes a hierarchical GLM
¹⁴⁹ likelihood (Lee and Nelder 1996; Wood 2017), making likelihood-based statistics for model
¹⁵⁰ comparison like AIC (Akaike 1974), AICc (Hoeting, Davis, Merton, and Thompson 2006), BIC
¹⁵¹ (Schwarz 1978), deviance (McCullagh and Nelder 1989), and likelihood ratio tests available.
¹⁵² These types of statistics are not available for quasi-likelihood (Wedderburn 1974; Breslow
¹⁵³ and Clayton 1993) or pseudo-likelihood approaches (Wolfinger and O'Connell 1993), which
¹⁵⁴ only specify the first two moments of a distribution. Next, we describe a brief overview of
¹⁵⁵ the approach and how it can be used for several primary data analysis tasks (Tredennick,
¹⁵⁶ Hooker, Ellner, and Adler 2021) like model comparison, parameter estimation, inference,
¹⁵⁷ model diagnostics, and prediction. Then in Section 3 and Section 4, we show how to use
¹⁵⁸ **spmodel** to carry out these primary data analysis tasks for various data sets.

159 2.1. Formulating the hierarchical likelihood

¹⁶⁰ We can write the SPGLM likelihood hierarchically as

$$[\mathbf{y}|\mathbf{X}, \varphi, \boldsymbol{\theta}] = \int_{\mathbf{w}} \int_{\boldsymbol{\beta}} [\mathbf{y}|f^{-1}(\mathbf{w}), \varphi] [\mathbf{w}|\mathbf{X}, \boldsymbol{\beta}, \boldsymbol{\theta}] d\boldsymbol{\beta} d\mathbf{w}, \quad (4)$$

¹⁶¹ where $[\mathbf{y}|f^{-1}(\mathbf{w}), \varphi]$ is the density for the appropriate response distribution of \mathbf{y} (e.g., bi-
¹⁶² nomial, Poisson) given the latent \mathbf{w} and dispersion parameter (φ), and $[\mathbf{w}|\mathbf{X}, \boldsymbol{\beta}, \boldsymbol{\theta}]$ is the

¹⁶³ multivariate Gaussian density for \mathbf{w} given the explanatory variables (\mathbf{X}), fixed effects ($\boldsymbol{\beta}$),
¹⁶⁴ and spatial covariance parameters ($\boldsymbol{\theta}$). The elements of $[\mathbf{y}|f^{-1}(\mathbf{w}), \varphi]$ are conditionally in-
¹⁶⁵ dependent (given \mathbf{w}), but the elements of $[\mathbf{w}|\mathbf{X}, \boldsymbol{\beta}, \boldsymbol{\theta}]$ share spatial covariance. Following
¹⁶⁶ Harville (1977), we can integrate $\boldsymbol{\beta}$ out of Equation 4, which yields

$$[\mathbf{y}|\mathbf{X}, \varphi, \boldsymbol{\theta}] = \int_{\mathbf{w}} [\mathbf{y}|f^{-1}(\mathbf{w}), \varphi][\mathbf{w}|\mathbf{X}, \boldsymbol{\theta}] d\mathbf{w}, \quad (5)$$

¹⁶⁷ where $[\mathbf{w}|\mathbf{X}, \boldsymbol{\theta}]$ is the restricted (i.e., residual) multivariate Gaussian density (Patterson and
¹⁶⁸ Thompson 1971) for \mathbf{w} given the explanatory variables and covariance parameters. Equation 5
¹⁶⁹ can synonymously be written after profiling the overall variance out of $\boldsymbol{\Sigma}$, which reduces the
¹⁷⁰ dimension of $\boldsymbol{\theta}$ by one for optimization (Wolfinger, Tobias, and Sall 1994). The restricted
¹⁷¹ multivariate Gaussian density is given by

$$[\mathbf{w}|\mathbf{X}, \boldsymbol{\theta}] = \frac{\exp(-\frac{1}{2}(\mathbf{y} - \mathbf{X}\tilde{\boldsymbol{\beta}})\boldsymbol{\Sigma}^{-1}(\mathbf{y} - \mathbf{X}\tilde{\boldsymbol{\beta}})^T)}{(2\pi)^{(n-p)/2}|\boldsymbol{\Sigma}|^{1/2}|\mathbf{X}^T\boldsymbol{\Sigma}^{-1}\mathbf{X}|^{1/2}},$$

¹⁷² where $\tilde{\boldsymbol{\beta}} = (\mathbf{X}^T\boldsymbol{\Sigma}^{-1}\mathbf{X})^{-1}\mathbf{X}^T\boldsymbol{\Sigma}^{-1}\mathbf{w}$ and $|\cdot|$ denotes the determinant. Next, let

$$\ell_{\mathbf{w}} = \log([\mathbf{y}|f^{-1}(\mathbf{w}), \varphi][\mathbf{w}|\mathbf{X}, \boldsymbol{\theta}])$$

¹⁷³ and rewrite Equation 5 as

$$[\mathbf{y}|\mathbf{X}, \varphi, \boldsymbol{\theta}] = \int_{\mathbf{w}} \exp(\ell_{\mathbf{w}}) d\mathbf{w}.$$

¹⁷⁴ A second-order Taylor series expansion of $\ell_{\mathbf{w}}$ around a point $\hat{\mathbf{w}}$ yields

$$[\mathbf{y}|\mathbf{X}, \varphi, \boldsymbol{\theta}] \approx \int_{\mathbf{w}} \exp(\ell_{\hat{\mathbf{w}}} + \mathbf{g}^T(\mathbf{w} - \hat{\mathbf{w}}) + \frac{1}{2}(\mathbf{w} - \hat{\mathbf{w}})^T \mathbf{G}(\mathbf{w} - \hat{\mathbf{w}})) d\mathbf{w},$$

¹⁷⁵ where \mathbf{g} and \mathbf{G} are the gradient and Hessian, respectively, of $\ell_{\mathbf{w}}$ with respect to \mathbf{w} . If $\hat{\mathbf{w}}$ is a
¹⁷⁶ value for which $\mathbf{g} = \mathbf{0}$,

$$[\mathbf{y}|\mathbf{X}, \varphi, \boldsymbol{\theta}] \approx \exp(\ell_{\hat{\mathbf{w}}}) \int_{\mathbf{w}} \exp(-\frac{1}{2}(\mathbf{w} - \hat{\mathbf{w}})^T (-\mathbf{G})(\mathbf{w} - \hat{\mathbf{w}})) d\mathbf{w}. \quad (6)$$

¹⁷⁷ The integral in Equation 6 can be solved by leveraging properties of the normalizing constant
¹⁷⁸ of a multivariate Gaussian distribution. Thus, rewriting $\exp(\ell_{\hat{\mathbf{w}}})$ yields

$$[\mathbf{y}|\mathbf{X}, \varphi, \boldsymbol{\theta}] \approx [\mathbf{y}|f^{-1}(\hat{\mathbf{w}}), \varphi][\hat{\mathbf{w}}|\mathbf{X}, \boldsymbol{\theta}] (2\pi)^{n/2} |-\mathbf{G}_{\hat{\mathbf{w}}}|^{-1/2}. \quad (7)$$

¹⁷⁹ Maximizing the natural logarithm of Equation 7 requires a doubly iterative process over
¹⁸⁰ $\boldsymbol{\theta}$ and φ as well as \mathbf{w} , eventually yielding the the marginal restricted maximum likelihood
¹⁸¹ estimators $\hat{\varphi}$ and $\hat{\boldsymbol{\theta}}$ and their corresponding values of $\hat{\mathbf{w}}$. Maximizing this log likelihood
¹⁸² requires repeatedly evaluating $\boldsymbol{\Sigma}^{-1}$, \mathbf{g} , and \mathbf{G} ; see Ver Hoef *et al.* (2024) for more details
¹⁸³ and comparisons to other approaches as well as and forms of \mathbf{g} and \mathbf{G} for various response
¹⁸⁴ distributions.

¹⁸⁵ 2.2. Estimating fixed effects

Though the fixed effects are integrated out of the likelihood, we can still estimate them using generalized least squares (GLS) principles, a common practice for linear models estimated using restricted maximum likelihood methods. Had we observed \mathbf{w} , a GLS estimator for β is given by

$$\hat{\beta} = (\mathbf{X}^\top \Sigma^{-1} \mathbf{X})^{-1} \mathbf{X}^\top \Sigma^{-1} \mathbf{w} = \mathbf{B} \mathbf{w},$$

where $\mathbf{B} = (\mathbf{X}^\top \Sigma^{-1} \mathbf{X})^{-1} \mathbf{X}^\top \Sigma^{-1}$. However, we only observe $\hat{\mathbf{w}}$, so it is reasonable to define $\hat{\beta} = \mathbf{B} \hat{\mathbf{w}}$. Thus, to derive properties of $\hat{\beta}$ like expectation and variance, we must derive these properties for $\hat{\mathbf{w}}$. To do so, we must condition on \mathbf{w} as if it were observed and invoke properties of the laws of total expectation and variance. Because $\hat{\mathbf{w}}$ was optimized via the likelihood, we assume that given \mathbf{w} , $\hat{\mathbf{w}}$ has mean \mathbf{w} and variance approximately equal to $-\mathbf{H}^{-1}$ (the inverse Hessian). It follows that $E(\hat{\mathbf{w}})$ is given by

$$E(\hat{\mathbf{w}}) = E(E(\hat{\mathbf{w}}|\mathbf{w})) = E(\mathbf{w}) = \mathbf{X}\beta$$

and $\text{Var}(\hat{\mathbf{w}})$ is given by

$$\begin{aligned} \text{Var}(\hat{\mathbf{w}}) &= E(\text{Var}(\hat{\mathbf{w}}|\mathbf{w})) + \text{Var}(E(\hat{\mathbf{w}}|\mathbf{w})) \\ &= E(-\mathbf{H}^{-1}) + \text{Var}(\mathbf{w}) \\ &= -\mathbf{H}^{-1} + \Sigma \end{aligned}$$

Putting this all together, it follows that

$$E(\hat{\beta}) = E(\mathbf{B} \hat{\mathbf{w}}) = \mathbf{B} E(\hat{\mathbf{w}}) = (\mathbf{X}^\top \Sigma^{-1} \mathbf{X})^{-1} (\mathbf{X}^\top \Sigma^{-1} \mathbf{X}) \beta = \beta$$

and

$$\begin{aligned} \text{Var}(\hat{\beta}) &= \text{Var}(\mathbf{B} \hat{\mathbf{w}}) \\ &= \mathbf{B} \text{Var}(\hat{\mathbf{w}}) \mathbf{B}^\top \\ &= \mathbf{B} (-\mathbf{H}^{-1} + \Sigma) \mathbf{B}^\top \\ &= \mathbf{B} (-\mathbf{H})^{-1} \mathbf{B}^\top + \mathbf{B} \Sigma \mathbf{B}^\top \\ &= \mathbf{B} (-\mathbf{H})^{-1} \mathbf{B}^\top + (\mathbf{X}^\top \Sigma^{-1} \mathbf{X})^{-1} \end{aligned}$$

In practice, $\text{Var}(\hat{\beta})$ is estimated by evaluating Σ at $\hat{\theta}$, the estimated covariance parameter vector.

These results are important because they justify closed-form solutions for $\hat{\beta}$ and its associated variance. Closed-form solutions are useful because they bypass the need for sampling-based strategies to evaluate the mean and variance of $\hat{\beta}$, a common technique for other approaches to SPGLMs like Bayesian MCMC.

2.3. Inspecting model diagnostics

Inspecting model diagnostics is an important step of the modeling process that can yield valuable insights into model behavior and unusual observations. Montgomery, Peck, and Vining (2021) contextualize three components of unusual observations: outliers, leverage, and influence. An observation is an outlier if it has an unusual response value relative to

expectation. The response GLM residuals simply compare the observation to its fitted latent mean:

$$\mathbf{r}_r = \mathbf{y} - f^{-1}(\hat{\mathbf{w}})$$

Because observations often have a unique support in a GLM (e.g., only two possible response values for binary data) and the variance of an observation generally depends on its mean, response residuals lack some utility. Deviance residuals are a function of response residuals that are appropriately scaled to behave more like response residuals in a standard linear model. Deviance residuals are given by

$$\mathbf{r}_d = sign(\mathbf{r}_r)\sqrt{\mathbf{d}},$$

where \mathbf{d} is a vector of individual deviances. The sum of the squared deviance residuals equals the sum of \mathbf{d} . The sum of \mathbf{d} is the deviance of the model fit, which quantifies twice the difference in log likelihoods between the a saturated model that fits every observation perfectly (i.e., $\mathbf{y} = f^{-1}(\hat{\mathbf{w}}_i)$ for all i) and the fitted model (Myers, Montgomery, Vining, and Robinson 2012). Deviance is often used as a fit statistic; lower values of deviance imply a better model fit. Pearson and standardized residuals are other types of GLM residuals that involve a scaling of the response residuals; the Pearson residuals scale \mathbf{r}_r by the square root of \mathbf{V} , while the standardized residuals scale the deviance residuals by $\frac{1}{\sqrt{(1-\mathbf{L}_{ii})}}$, where \mathbf{L}_{ii} is the i th diagonal element of the leverage matrix, which we discuss next.

An observation has high leverage if its combination of explanatory variables is far away from other observations. In a linear model, the leverage (i.e., hat) values are the diagonal of the leverage (i.e., projection, hat) matrix, $\mathbf{L} = \mathbf{X}(\mathbf{X}^\top \mathbf{X})^{-1}\mathbf{X}^\top$. In a GLM, the leverage matrix is given by

$$\mathbf{L} = \mathbf{V}^{1/2} \mathbf{X} (\mathbf{X}^\top \mathbf{V} \mathbf{X})^{-1} \mathbf{X}^\top \mathbf{V}^{1/2},$$

where \mathbf{V} is a diagonal matrix with i th diagonal element equal to the variance of the response distribution evaluated at $f^{-1}(\mathbf{w}_i)$ (Faraway 2016); \mathbf{V} is sometimes called the GLM weight matrix. The larger the value of \mathbf{L}_{ii} , the more severe the leverage from the i th observation.

An observation is influential if it has a sizable impact on model fit. Influence is measured using Cook's distance (Cook 1979; Cook and Weisberg 1982), which is given for a GLM by

$$\mathbf{c} = \frac{\mathbf{r}_s^2}{\text{tr}(\mathbf{L})} \frac{diag(\mathbf{L})}{(1 - diag(\mathbf{L}))},$$

where \mathbf{r}_s^2 are the standardized residuals and $diag(\mathbf{L})$ indicates the diagonal elements of the leverage matrix. The larger the value of \mathbf{c}_i , the more severe the influence from the i th observation. Montgomery *et al.* (2021) provide guidance for interpreting these types of statistics, including cutoffs to consider when identifying unusual residual, leverage, or influence values.

In a linear model, the R^2 (R-squared) statistic quantifies the proportion of variability in the data captured by the explanatory variables. It is calculated as one minus the ratio of the error sum of squares to the total sum of squares (Rencher and Schaalje 2008). In a GLM, there are many ways to define a statistic that emulates the aforementioned meaning of R^2 from the linear model (Smith and McKenna 2013). This statistic is called a pseudo R-squared (PR^2).

²⁴⁴ One PR^2 for GLMs simply replaces the sums of squares ratio from the linear model with the
²⁴⁵ deviance ratio:

$$PR^2 = 1 - \frac{deviance_{fit}}{deviance_{null}},$$

²⁴⁶ where $deviance_{fit}$ is the deviance of the fitted model (sometimes called the residual deviance)
²⁴⁷ and $deviance_{null}$ is the deviance of the model taking $\mathbf{X} \equiv \mathbf{1}$, a column of all ones (i.e., an
²⁴⁸ intercept-only model). In practice, $deviance_{null}$ is derived by computing $\hat{\mathbf{w}}$ when $\mathbf{X} \equiv \mathbf{1}$ given
²⁴⁹ $\hat{\boldsymbol{\theta}}$ and $\hat{\varphi}$ from the fitted model. Like R^2 , PR^2 can be adjusted to account for the numbers
²⁵⁰ of parameters estimated in a model. Because the $deviance_{null}$ denominator changes across
²⁵¹ fitted models (as the values of $\hat{\boldsymbol{\theta}}$ and $\hat{\varphi}$ change), this statistic should not be used as a model
²⁵² comparison tool. Rather, it should be used as an informative diagnostic tool that unique
²⁵³ to each model fit and describes how much variability from that model is attributable to the
²⁵⁴ explanatory variables.

²⁵⁵ 2.4. Predicting at new locations

²⁵⁶ We may also predict values of the latent mean (on the link scale) at new locations by leveraging
²⁵⁷ the spatial covariance between observed locations and new locations (spatial prediction is
²⁵⁸ also called Kriging; see [Cressie \(1990\)](#)). Again suppose that we observed \mathbf{w} and we want to
²⁵⁹ make predictions at \mathbf{u} , a vector of latent means at the new locations that follows the same
²⁶⁰ SPGLM from Equation 3 and having fixed effects design matrix, \mathbf{X}_u . The vector $(\mathbf{w}, \mathbf{u})^\top$
²⁶¹ has expectation $(\mathbf{X}\boldsymbol{\beta}, \mathbf{X}_u\boldsymbol{\beta})^\top$ and covariance matrix $\begin{bmatrix} \boldsymbol{\Sigma} & \boldsymbol{\Sigma}_{wu} \\ \boldsymbol{\Sigma}_{uw} & \boldsymbol{\Sigma}_{uu} \end{bmatrix}$, where $\boldsymbol{\Sigma} = \text{Var}(\mathbf{w}, \mathbf{w})$,
²⁶² $\boldsymbol{\Sigma}_{wu} = \text{Var}(\mathbf{w}, \mathbf{u})$, $\boldsymbol{\Sigma}_{uw} = \boldsymbol{\Sigma}_{wu}^\top$ and $\boldsymbol{\Sigma}_{u,u} = \text{Var}(\mathbf{u}, \mathbf{u})$. By assumption, we have observed \mathbf{w} ,
²⁶³ so we may derive the conditional distribution of $\mathbf{u}|\mathbf{w}$, which has the following properties:

$$\begin{aligned} E(\mathbf{u}|\mathbf{w}) &= \mathbf{X}_u\boldsymbol{\beta} + \boldsymbol{\Sigma}_{u,w}\boldsymbol{\Sigma}^{-1}(\mathbf{w} - \mathbf{X}\boldsymbol{\beta}) \\ \text{Var}(\mathbf{u}|\mathbf{w}) &= \boldsymbol{\Sigma}_{u,u} - \boldsymbol{\Sigma}_{u,w}\boldsymbol{\Sigma}^{-1}\boldsymbol{\Sigma}_{w,u} \end{aligned}$$

²⁶⁴ [Ver Hoef et al. \(2024\)](#) show how these equations are adjusted to reflect uncertainty in both
²⁶⁵ $\hat{\boldsymbol{\beta}}$ and $\hat{\mathbf{w}}$ while leveraging the laws of total expectation and variance yet again. They derive
²⁶⁶ the predictor of \mathbf{u} , $\hat{\mathbf{u}}$, and its associated variance, given by:

$$\begin{aligned} \hat{\mathbf{u}} &= \mathbf{X}_u\hat{\boldsymbol{\beta}} + \boldsymbol{\Sigma}_{u,w}\boldsymbol{\Sigma}^{-1}(\hat{\mathbf{w}} - \mathbf{X}\hat{\boldsymbol{\beta}}) \\ \text{Var}(\hat{\mathbf{u}}) &= \boldsymbol{\Sigma}_{u,u} - \boldsymbol{\Sigma}_{u,w}\boldsymbol{\Sigma}^{-1}\boldsymbol{\Sigma}_{w,u} + \mathbf{K}(\mathbf{X}^\top\boldsymbol{\Sigma}^{-1}\mathbf{X})^{-1}\mathbf{K}^\top + \boldsymbol{\Lambda}(-\mathbf{H})^{-1}\boldsymbol{\Lambda}^\top, \end{aligned}$$

²⁶⁷ where $\mathbf{K} = \mathbf{X}_u - \boldsymbol{\Sigma}_{u,w}\boldsymbol{\Sigma}^{-1}\mathbf{X}$ and $\boldsymbol{\Lambda} = \mathbf{X}_u\mathbf{B} + \boldsymbol{\Sigma}_{u,w}\boldsymbol{\Sigma}^{-1}(\mathbf{1} - \mathbf{X}\mathbf{B})$ for a vector of ones, $\mathbf{1}$. As
²⁶⁸ with $\hat{\boldsymbol{\beta}}$, in practice these covariance matrices are evaluated at $\hat{\boldsymbol{\theta}}$.

3. Modeling moose presence in Alaska, USA

²⁶⁹ The `moose` data in **spmodel** contain information on moose (*Alces Alces*) presence in the Togiak
²⁷⁰ region of Alaska, USA. `moose` is an `sf` object, a special data frame that is supplemented with
²⁷¹ spatial information using the `sf` package in R ([Pebesma 2018](#)). The first few rows of `moose`
²⁷² look like:

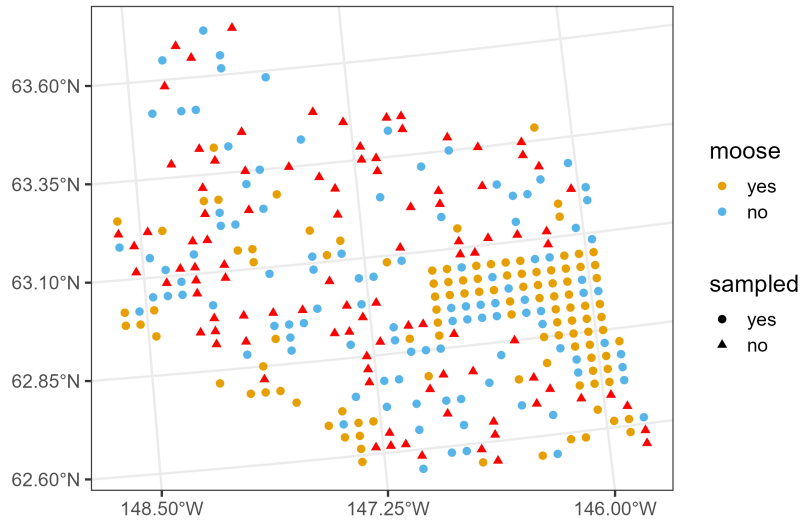


Figure 3: Moose presence in Alaska. Circles represent moose presence or absence (based on color) and triangles represent locations at which moose presence probability predictions are desired.

```
R> head(moose)
```

```
Simple feature collection with 6 features and 4 fields
Geometry type: POINT
Dimension: XY
Bounding box: xmin: 281896.4 ymin: 1518398 xmax: 311325.3 ymax: 1541016
Projected CRS: NAD83 / Alaska Albers
# A tibble: 6 x 5
  elev strat count presence      geometry
  <dbl> <chr> <dbl> <fct>       <POINT [m]>
1 469. L     0 0   no          (293542.6 1541016)
2 362. L     0 0   no          (298313.1 1533972)
3 173. M     0 0   no          (281896.4 1532516)
4 280. L     0 0   no          (298651.3 1530264)
5 620. L     0 0   no          (311325.3 1527705)
6 164. M     0 0   no          (291421.5 1518398)
```

273 There are five columns: `elev`, the numeric site elevation (meters); `strat` a stratification
 274 variable for sampling with two levels, "L" and "M", which are categorized by landscape metrics
 275 at each site; `count`, the number of moose at each site; `presence`, a factor that indicates
 276 whether at least one moose was observed at each site (0 implies no moose; 1 implies at least
 277 one moose); and `geometry`, the NAD83/Alaska Albers (EPSG: 3338) projected coordinate of
 278 each site (these data are point-referenced because each observation occurs at point coordinates
 279 and are represented by a POINT geometry. Moose are most prevalent in the southwestern and
 280 eastern parts of the Togiak region (Figure 3).

281 The `moose_preds` data in `spmodel` is an `sf` object with point locations at which moose
 282 presence predictions are desired. Like `moose`, `moose_preds` contains `elev` and `strat` for each

283 site:

```
R> head(moose_preds)

Simple feature collection with 6 features and 2 fields
Geometry type: POINT
Dimension:      XY
Bounding box:  xmin: 291839.8 ymin: 1436192 xmax: 401239.6 ymax: 1512103
Projected CRS: NAD83 / Alaska Albers
# A tibble: 6 x 3
  elev strat      geometry
  <dbl> <chr>    <POINT [m]>
1 143. L      (401239.6 1436192)
2 324. L      (352640.6 1490695)
3 158. L      (360954.9 1491590)
4 221. M      (291839.8 1466091)
5 209. M      (310991.9 1441630)
6 218. L      (304473.8 1512103)
```

284 **3.1. Model Fitting**

285 SPGLMs in **spmodel** are fit using the **spglm()** function. The **spglm()** function requires
 286 four arguments: **formula**, the relationship between the response and explanatory variables;
 287 **family**, the response distribution assumed for the response variable; **data**, the data frame
 288 that contains the variables in **formula**, and **spcov_type**, the type of spatial covariance.
 289 The **formula**, **family**, and **data** arguments are the three required arguments to **glm()** for
 290 nonspatial GLMs. So, the transition from **glm()** to **spglm()** simply requires one additional
 291 argument: **spcov_type**. When **data** is not an **sf** object, **spglm()** also requires the **xcoord**
 292 and **ycoord** arguments, which indicate the columns in **data** that represent the projected x-
 293 and y-coordinates, respectively.

294 We use **spglm()** to fit a spatial GLM (i.e., here, a spatial logistic regression) quantifying the
 295 effect of elevation and strata on moose presence:

```
R> spbin <- spglm(
+   formula = presence ~ elev + strat,
+   family = binomial,
+   data = moose,
+   spcov_type = "exponential"
+ )
```

296 The **summary()** function returns a model summary that returns relevant information like the
 297 function call, deviance residuals, a coefficients table of fixed effects, the pseudo R-squared,
 298 spatial covariance parameters, and the GLM dispersion parameter (fixed at one in logistic
 299 regression):

```
R> summary(spbin)
```

```

Call:
spglm(formula = presence ~ elev + strat, family = binomial, data = moose,
      spcov_type = "exponential")

Deviance Residuals:
    Min      1Q  Median      3Q     Max 
-1.7535 -0.8005  0.3484  0.7893  1.5797 

Coefficients (fixed):
            Estimate Std. Error z value Pr(>|z|)    
(Intercept) -2.465713   1.486212 -1.659 0.097104 .  
elev         0.006036   0.003525  1.712 0.086861 .  
stratM       1.439273   0.420591  3.422 0.000622 *** 
---
Signif. codes:  0 '***' 0.001 '**' 0.01 '*' 0.05 '.' 0.1 ' ' 1

Pseudo R-squared: 0.06275

Coefficients (exponential spatial covariance):
      de        ie      range
5.145e+00 1.294e-03 4.199e+04

Coefficients (Dispersion for binomial family):
dispersion
      1

```

- 300 The model suggests that elevation is positively associated with the log odds of moose presence
 301 (p -value ≈ 0.087), after controlling for strata. The model also suggests that moose have a
 302 higher log odds of presence in the "M" strata compared to the "L" strata (p -value < 0.001),
 303 after controlling for elevation.
- 304 The fixed effects coefficients table from `summary()` is often of primary scientific interest, but
 305 it is not immediately usable when printed directly to the R console. The `tidy()` function
 306 tidies this table, turning it into a data frame (i.e., a tibble) with standard column names:

```

R> tidy(spbin, conf.int = TRUE)

# A tibble: 3 x 7
  term      estimate std.error statistic p.value conf.low conf.high
  <chr>      <dbl>     <dbl>     <dbl>    <dbl>    <dbl>     <dbl>
1 (Intercept) -2.47      1.49     -1.66  0.0971   -5.38e+0   0.447
2 elev        0.00604   0.00353     1.71  0.0869   -8.73e-4   0.0129
3 stratM      1.44       0.421     3.42  0.000622  6.15e-1    2.26

```

307 **3.2. Model Comparison**

308 The strength of spatial covariance in the data affects how beneficial an SPGLM is relative to
 309 a GLM. When the spatial covariance is strong, the SPGLM should notably outperform the
 310 GLM. When the spatial covariance is weak, the SPGLM and GLM should perform similarly.
 311 We can quantify the benefits of incorporating spatial covariance for a particular data set
 312 by comparing the fit of a SPGLM to a GLM. We can fit a GLM in **spmodel** by specifying
 313 `spcov_type = "none"`:

```
R> bin <- spglm(
+   formula = presence ~ elev + strat,
+   family = binomial,
+   data = moose,
+   spcov_type = "none"
+ )
```

314 While the `spglm()` approach evaluates the HGLMM likelihood with $\sigma_{de}^2 = 0$ and $\sigma_{ie}^2 \approx 0$
 315 instead of just the GLM likelihood, the parameter estimates and their standard errors are the
 316 same:

```
R> bin_glm <- glm(
+   formula = presence ~ elev + strat,
+   family = binomial,
+   data = moose,
+ )
R> round(coef(bin), digits = 4)

(Intercept)      elev      stratM
-0.4247     -0.0003     0.8070

R> round(coef(bin_glm), digits = 4)

(Intercept)      elev      stratM
-0.4247     -0.0003     0.8070

R> round(sqrt(diag(vcov(bin))), digits = 4)

(Intercept)      elev      stratM
  0.4208     0.0019     0.2906

R> round(sqrt(diag(vcov(bin_glm))), digits = 4)

(Intercept)      elev      stratM
  0.4208     0.0019     0.2906
```

317 However, using `spglm()` instead of `glm()` ensures that **spmodel** helper functions are available
 318 and that each of the `spglm()` models uses the same likelihood:

```
R> glance(spbin)

# A tibble: 1 x 10
      n     p   npar value    AIC   AICc    BIC logLik deviance
  <int> <dbl> <int> <dbl> <dbl> <dbl> <dbl> <dbl>
1    218     3     3  676.  682.  683.  693. -338.     176.
# i 1 more variable: pseudo.r.squared <dbl>

R> glance(bin)

# A tibble: 1 x 10
      n     p   npar value    AIC   AICc    BIC logLik deviance
  <int> <dbl> <int> <dbl> <dbl> <dbl> <dbl> <dbl>
1    218     3     0  708.  708.  708.  708. -354.     294.
# i 1 more variable: pseudo.r.squared <dbl>
```

319 The likelihood-based statistics AIC, AICc, BIC, and deviance are much lower for the SPGLM,
 320 indicating a better fit relative to the GLM. We may also perform a likelihood ratio test (LRT)
 321 between the two models, as the GLM is a special case of the SPGLM (i.e., is nested within
 322 the SPGLM):

```
R> anova(spbin, bin)

Likelihood Ratio Test

Response: presence
          Df Chi2 Pr(>Chi2)
spbin vs bin  3 31.546 6.525e-07 ***
---
Signif. codes:  0 '***' 0.001 '**' 0.01 '*' 0.05 '.' 0.1 ' ' 1
```

323 The LRT provides strong evidence that the SPGLM is preferred to the GLM (*p*-value <
 324 0.001).

325 An alternative approach to model comparison is to use a cross-validation procedure (James,
 326 Witten, Hastie, and Tibshirani 2013). The `loocv()` function performs leave-one-out cross
 327 validation, comparing the predicted mean (on the response scale) to the observed response
 328 variable for each hold-out observation, recomputing estimates of β in each iteration. Per-
 329 forming leave-one-out cross validation tends to be more computationally efficient than fitting
 330 the model, as leave-one-out cross validation requires only one set of products involving the in-
 331 verse covariance matrix (the primary computational burden), while fitting traditional models
 332 requires these products for each optimization iteration. After performing leave-one-out cross
 333 validation, statistics like bias, mean-squared-prediction error (MSPE), and the square root of
 334 MSPE (RMSPE) can be used to evaluate models:

```
R> loocv(spbin)
```

```
# A tibble: 1 x 3
  bias  MSPE RMSPE
  <dbl> <dbl> <dbl>
1 0.0000206 0.156 0.394
```

R> loocv(bin)

```
# A tibble: 1 x 3
  bias  MSPE RMSPE
  <dbl> <dbl> <dbl>
1 -1.23e-9 0.240 0.490
```

- 335 Both models have negligible bias, but the SPGLM has much lower MSPE and RMSPE than
 336 the GLM, indicating the SPGLM predictions are far more efficient. Three separate metrics
 337 (likelihood-based statistics, likelihood-ratio test, and leave-one-out cross validation) prefer
 338 the SPGLM to the GLM.
- 339 We can compare two SPGLMs with different spatial covariance functions using likelihood-
 340 based statistics and leave-one-out cross validation, but we can't use the LRT because generally,
 341 the spatial covariance functions are not nested:

```
R> spbin2 <- update(spbin, spcov_type = "gaussian")
R> glances(spbin, spbin2)
```

```
# A tibble: 2 x 11
  model      n     p   npar value    AIC   AICc    BIC logLik deviance
  <chr>  <int> <dbl> <int> <dbl> <dbl> <dbl> <dbl> <dbl> <dbl>
1 spbin2    218     3     3  674.  680.  680.  690. -337.    198.
2 spbin     218     3     3  676.  682.  682.  693. -338.    176.
# i 1 more variable: pseudo.r.squared <dbl>
```

R> loocv(spbin)

```
# A tibble: 1 x 3
  bias  MSPE RMSPE
  <dbl> <dbl> <dbl>
1 0.0000206 0.156 0.394
```

R> loocv(spbin2)

```
# A tibble: 1 x 3
  bias  MSPE RMSPE
  <dbl> <dbl> <dbl>
1 -0.000261 0.146 0.382
```

- 342 The "exponential" spatial covariance (**spbin**) has a slightly lower (better) deviance but
 343 slightly higher (worse) AIC, AICc, and BIC than the "gaussian" spatial covariance (**spbin2**).

- ³⁴⁴ Both spatial covariance functions have similar leave-one-out cross validation metrics, though
³⁴⁵ the "gaussian" spatial covariance RMSPE is slightly lower (better). For practical purposes,
³⁴⁶ these models fit similarly.
- ³⁴⁷ Frequently in spatial statistics, the difference in model fit between the best spatial model
³⁴⁸ and worst spatial model is much smaller than the difference in model fit between the worst
³⁴⁹ spatial model and the nonspatial model, implying that accounting for some form of spatial
³⁵⁰ covariance is very beneficial. Two spatial covariance functions to consider starting with are the
³⁵¹ exponential and Gaussian, which have quite different origin behaviors (Figure 2), something
³⁵² Stein (1999) argues is important to characterize accurately.

³⁵³ 3.3. Model Diagnostics

- ³⁵⁴ `spmodel` provides a suite of tools for model diagnostics. One is `augment()`, which augments
³⁵⁵ the data used in the model with several model diagnostics (introduced in Section 2.3):

```
R> augment(spbin)

Simple feature collection with 218 features and 8 fields
Geometry type: POINT
Dimension:      XY
Bounding box:  xmin: 269085 ymin: 1416151 xmax: 419057.4 ymax: 1541016
Projected CRS: NAD83 / Alaska Albers
# A tibble: 218 x 9
   presence elev strat .fitted .resid     .hat   .cooksdi .std.resid
   * <fct>    <dbl> <chr>   <dbl>  <dbl>   <dbl>    <dbl>
 1 0        469. L     -1.95 -0.516  0.0476  0.00465  -0.528
 2 0        362. L     -2.70 -0.361  0.0123  0.000548  -0.363
 3 0        173. M     -1.96 -0.514  0.00455  0.000405  -0.516
 4 0        280. L     -3.15 -0.290  0.00413  0.000117  -0.291
 5 0        620. L     -1.19 -0.728  0.168   0.0427   -0.798
 6 0        164. M     -1.71 -0.576  0.00534  0.000598  -0.578
 7 0        164. M     -1.60 -0.606  0.00576  0.000714  -0.608
 8 0        186. L     -2.50 -0.397  0.00439  0.000233  -0.398
 9 0        362. L     -1.88 -0.532  0.0239  0.00237   -0.539
10 0       430. L     -1.54 -0.623  0.0497  0.00713  -0.639
# i 208 more rows
# i 1 more variable: geometry <POINT [m]>
```

- ³⁵⁶ The fitted values (`.fitted`) can be returned on either the link ($\hat{\mathbf{w}}$) or response ($f^{-1}(\hat{\mathbf{w}})$)
³⁵⁷ scale and the residuals (`.resid`) can be deviance, Pearson, or response residuals. The default
³⁵⁸ fitted values are on the link scale and the default residuals are deviance residuals. Also
³⁵⁹ returned by `augment()` are the leverage (`.hat`), Cook's distance (`.cooksdi`), and standardized
³⁶⁰ residuals `.std.resid` described in Section 2.3. A benefit of using `augment()` when `data` is
³⁶¹ an `sf` object is that the output is also an `sf` object, which makes it straightforward to create
³⁶² spatial diagnostic plots (Figure 4). Standard R helpers (e.g., `fitted()`, `residuals()`) are
³⁶³ also available to extract model diagnostics from the model object.

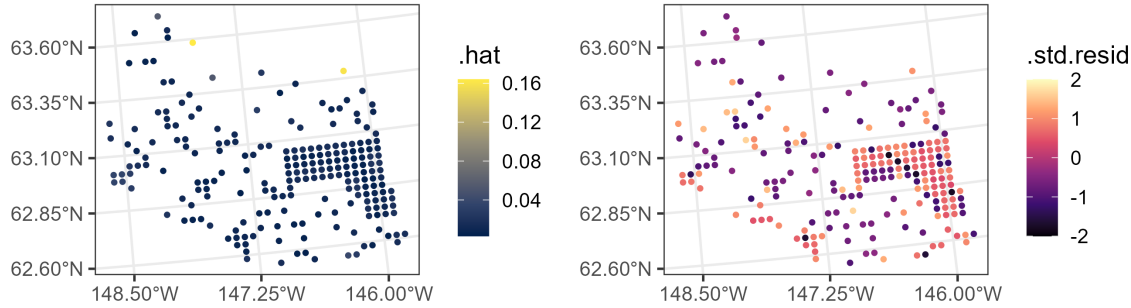


Figure 4: Moose presence model diagnostics, including leverage values (left) and standardized residuals (right).

364 The `plot()` function can also be used to return similar diagnostics as from `lm()` and `glm()`,
365 with additional tools for diagnosing spatial covariance. For example, we can inspect Cook's
366 distance values and the empirical spatial covariance as a function of distance with (Figure 5):

```
R> plot(spbin, which = c(4, 7))
```

367 The `varcomp()` function partitions model variability into several different components, help-
368 ing to elucidate the model's structure:

```
R> varcomp(spbin)
```

```
# A tibble: 3 x 2
  varcomp      proportion
  <chr>          <dbl>
1 Covariates (PR-sq) 0.0627
2 de             0.937
3 ie             0.000236
```

369 The pseudo R-squared (PR^2) is reported in the first row. The remaining variability ($1 - PR^2$)
370 is allocated proportionally to `de` and `ie` according to σ_{de}^2 and σ_{ie}^2 . This variability partitioning
371 is a useful tool that helps quantify how much the explanatory variables, residual spatial
372 variance, and residual nonspatial variance contribute to model fit, but as with PR^2 , should
373 not be used as a model comparison tool.

374 3.4. Prediction

375 We can predict the probability of moose presence at the locations in `moose_preds` using
376 `predict()`:

```
R> predict(spbin, newdata = moose_preds)[1:5]
```

1	2	3	4	5
0.06664165	-0.79069107	-1.60387940	-0.83159357	1.38183928

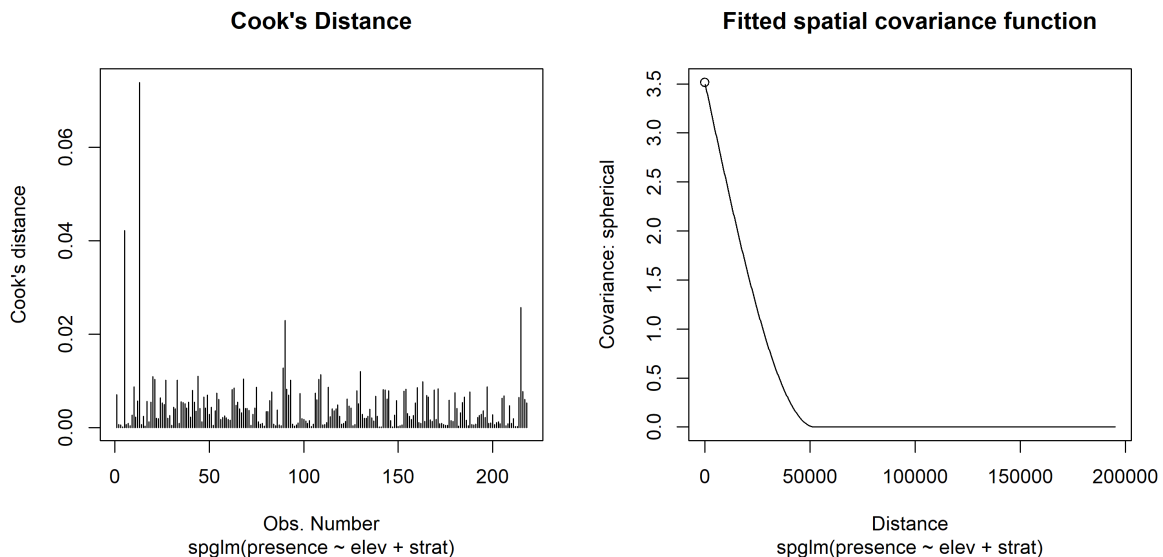


Figure 5: Moose presence model diagnostics, including Cook's distance (left) and the fitted spatial covariance as a function of distance (right).

377 By default, predictions are returned on the link scale, but this can be changed to the response
378 scale via `type`:

```
R> predict(spbin, newdata = moose_preds, type = "response")[1:5]
```

1	2	3	4	5
0.5166542	0.3120203	0.1674401	0.3033082	0.7992862

379 Predictions on the response scale are visualized alongside the fitted values ($f^{-1}(\hat{\mathbf{w}})$) in
380 Figure 6.

381 Prediction intervals for the probability of moose presence (on the link scale) are returned by
382 supplying `interval`:

```
R> predict(spbin, newdata = moose_preds, interval = "prediction")[1:5, ]
```

	fit	lwr	upr
1	0.06664165	-2.0374370	2.1707203
2	-0.79069107	-3.4758514	1.8944692
3	-1.60387940	-4.0953329	0.8875741
4	-0.83159357	-3.0704818	1.4072947
5	1.38183928	-0.7692107	3.5328893

383 We can alternatively use `augment()` to augment the prediction data with predictions. Argu-
384 ments to `predict()` can also be passed to `augment()`:

```
R> augment(spbin, newdata = moose_preds, interval = "prediction")
```

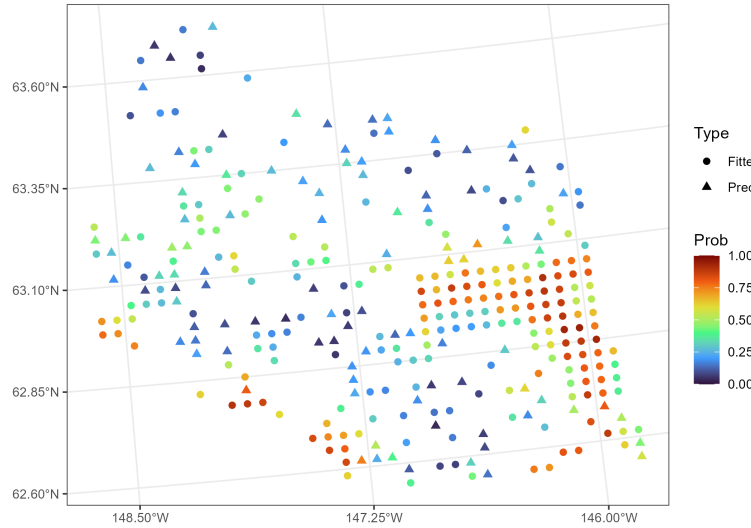


Figure 6: Moose presence probability fitted values and predictions. Fitted values are represented by circles and predictions by triangles.

```

Simple feature collection with 100 features and 5 fields
Geometry type: POINT
Dimension:     XY
Bounding box:  xmin: 269386.2 ymin: 1418453 xmax: 419976.2 ymax: 1541763
Projected CRS: NAD83 / Alaska Albers
# A tibble: 100 x 6
  elev strat .fitted .lower .upper      geometry
* <dbl> <chr>   <dbl>  <dbl>  <dbl>      <POINT [m]>
 1 143. L     0.0666 -2.04   2.17 (401239.6 1436192)
 2 324. L    -0.791  -3.48   1.89 (352640.6 1490695)
 3 158. L    -1.60   -4.10   0.888 (360954.9 1491590)
 4 221. M    -0.832  -3.07   1.41 (291839.8 1466091)
 5 209. M     1.38   -0.769  3.53 (310991.9 1441630)
 6 218. L    -2.59   -5.20   0.0177 (304473.8 1512103)
 7 127. L    -2.73   -5.24  -0.220 (339011.1 1459318)
 8 122. L    -2.32   -4.74   0.0920 (342827.3 1463452)
 9 191. L    -1.17   -4.01   1.66 (284453.8 1502837)
10 105. L    -0.905  -3.05   1.24 (391343.9 1483791)
# i 90 more rows

```

³⁸⁵ By using `augment()` when `newdata` is an `sf` object, predictions and their corresponding
³⁸⁶ uncertainties are readily available for spatial mapping (Figure 7).

4. Additional applications

³⁸⁷ Throughout the remainder of this section, we briefly highlight some additional **spmodel** ca-
³⁸⁸ pabilities for SPGLMs. In Section 4.1, we fit Poisson and negative binomial models with

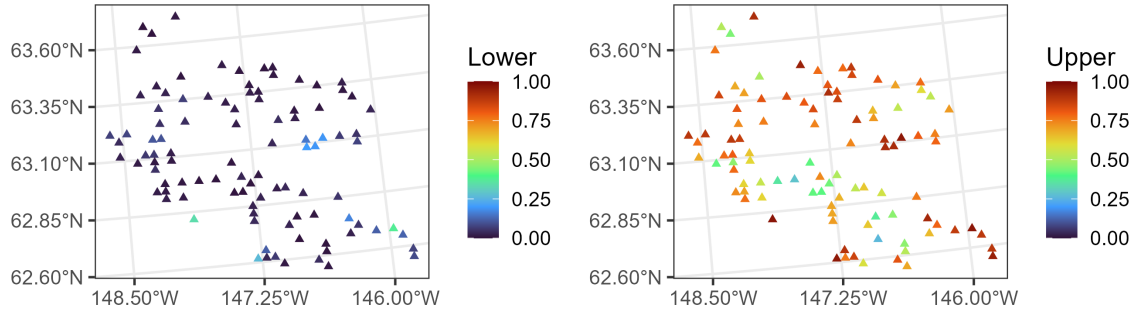


Figure 7: Moose presence 95% prediction interval lower bounds (left) and upper bounds (right).

Section	Data	Family	Geometry	Additional Features
4.1	Moose Counts	Poisson NBinomial	Point	Geometric Anisotropy
4.2	Lake Conductivity	Gamma	Point	Partition Factor ANOVA Contrasts
4.3	Harbor Seals	Binomial	Areal	Nonspatial Random Effects
4.4	Texas Voter Turnout	Beta	Point Areal	Likelihood-Ratio Test

Table 1: Section number, data set, family, geometry type, and additional features for each application.

and without geometric anisotropy for the point-referenced moose count data. In Section 4.2, we fit a Gamma model to the point-referenced lake conductivity data, showing how to fit a model with a partition factor, perform a spatial analysis of variance (ANOVA), fit contrasts for models with interactions. In Section 4.3, we fit a binomial model to the areal harbor seal trend data with a nonspatial random effect. Finally in Section 4.4, we fit beta models to Texas voter turnout data, which can be treated as point-referenced or areal, and use maximum likelihood to compare two models with different explanatory variables. Table 1 outlines the section number, data set, family (i.e., response distribution), geometry type, and additional **spmodel** features for each application.

4.1. Modeling moose counts in Alaska, USA

In addition to moose presence, moose counts are also recorded in `moose` (Figure 8). The Poisson and negative binomial response distributions can be used to model SPGLMs for count data. The Poisson distribution mean is equal to its variance, while the negative binomial has an extra parameter to accommodate overdispersion (where the variance is larger than the mean). Using a spherical spatial covariance function, we may fit both a Poisson and negative binomial SPGLM changing the `family` argument:

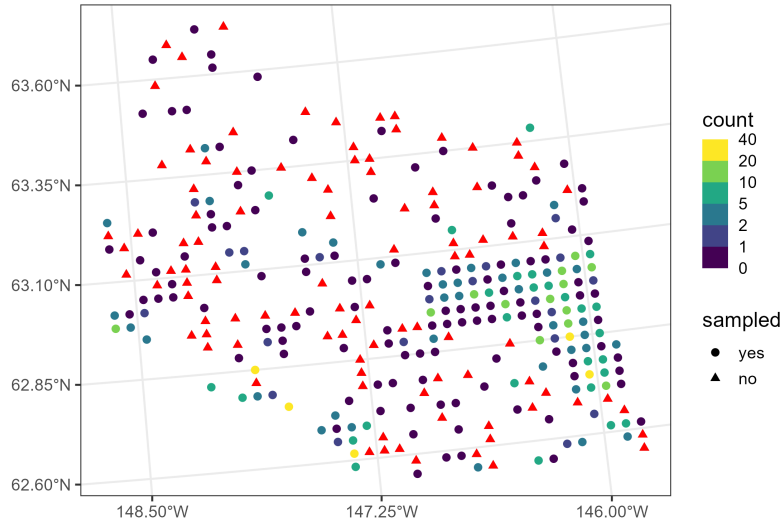


Figure 8: Moose counts in Alaska. Circles represent moose counts (based on color) and triangles represent locations at which mean count predictions are desired.

```
R> sppois <- spglm(
+   formula = count ~ elev + strat,
+   family = poisson,
+   data = moose,
+   spcov_type = "spherical"
+ )
R> spnb <- update(sppois, family = nbinomial)
```

Because the Poisson and negative binomial distributions have the same support (nonnegative integers), we can compare them using AIC, AICc, or BIC:

```
R> BIC(sppois, spnb)
```

	df	BIC
sppois	3	1344.574
spnb	4	1343.105

Implicit in our spatial covariance functions thus far has been an assumption of geometric isotropy. A spatial covariance function is geometrically isotropic if it decays with distance at the same rate in all directions (Figure 9; left). A spatial covariance is geometrically anisotropic if it decays with distance at different rates in different directions (Figure 9; right). Geometric anisotropy is formally incorporated by rotating and scaling original coordinates, yielding transformed coordinates that are geometrically isotropic:

$$\begin{bmatrix} x^* \\ y^* \end{bmatrix} = \begin{bmatrix} 1 & 0 \\ 0 & 1/\omega \end{bmatrix} \begin{bmatrix} \cos(\alpha) & \sin(\alpha) \\ -\sin(\alpha) & \cos(\alpha) \end{bmatrix} \begin{bmatrix} x \\ y \end{bmatrix}.$$

The parameters ω and α controls the scaling and rotation, respectively, of the major and minor axes of a level curve of equal spatial covariance (Figure 9). Using these transformed

415 coordinates, the partial sill (σ_{de}^2), nugget (σ_{ie}^2), and range (ϕ) parameters are estimated. We
 416 accommodate geometric anisotropy by supplying `anisotropy`:

```
R> sppois_anis <- update(sppois, anisotropy = TRUE)
R> spnb_anis <- update(spnb, anisotropy = TRUE)
```

417 According to BIC, the spatial negative binomial model with geometric anisotropy performs
 418 best:

```
R> BIC(sppois, spnb, sppois_anis, spnb_anis)
```

	df	BIC
sppois	3	1344.574
spnb	4	1343.105
sppois_anis	5	1341.143
spnb_anis	6	1339.714

419 The `plot()` function can be used to visualize the anisotropy (Figure 9):

```
R> plot(spnb, which = 8)
R> plot(spnb_anis, which = 8)
```

420 The spatial covariance is strongest in a northwest-southeast direction and weakest in the
 421 northeast-southwest direction (Figure 9), which is intuitive given the similar patterns in moose
 422 counts from Figure 8.

423 4.2. Modeling lake conductivity in Southwest, USA

424 The `lake` data in `spmodel` contains climate and chemical data for several lakes in four south-
 425 western states in the United States: Arizona, Colorado, Nevada, and Utah. We desire an
 426 SPGLM that characterizes the effect of temperature, state, and lake origin (whether the lake
 427 is naturally occurring or human made) on lake conductivity. Conductivity is a measure of
 428 dissolved ions (measured here in water), which is important for various physical, chemical,
 429 and biological processes. Chemical data are often heavily right-skewed, so we model them
 430 using an SPGLM assuming a Gamma distribution for the response. The `log_cond` variable
 431 in `lake` is the logarithm of conductivity, which we dynamically exponentiate within `formula`
 432 so that it is on the original scale:

```
R> spgam <- spglm(
+   formula = exp(log_cond) ~ temp * state + origin,
+   family = "Gamma",
+   data = lake,
+   spcov_type = "cauchy",
+   partition_factor = ~ year
+ )
```

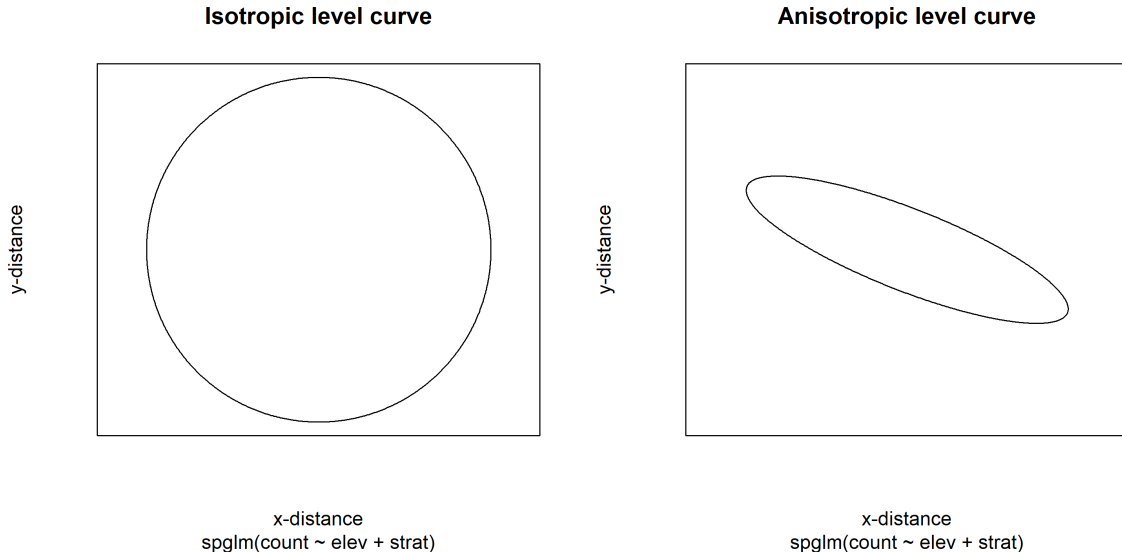


Figure 9: Level curves of equal spatial covariance for the negative binomial moose count models. The ellipse is centered at zero distance in the x-direction and y-direction, and points along the ellipse have equal levels of spatial covariance. In the isotropic level curve (left), spatial covariance decays equally in all directions. In the anistropic level curve (right), spatial covariance decays fastest in the northeast-southwest direction and slowest in the northwest-southeast direction (this pattern can be seen in the observed counts).

433 We model conductivity as a function of temperature, state, and lake origin, and we allow the
 434 effect of temperature to vary by state (`temp:state`). The `year` partition factor (specified via
 435 `partition_factor`) restricts spatial covariance to be nonzero only for observations sampled
 436 during the same year. Data were collected in 2012 and 2017, so this partition factor assumes
 437 independence between observations in 2012 and 2017. While we used the partition factor here
 438 illustratively, more generally, the utility of partition factors can be highly context dependent.
 439 When categorical variables have more than two levels, the default reference group contrasts
 440 are not well-suited to assess the variable's overall significance:

```
R> summary(spgam)
```

Call:

```
spglm(formula = exp(log_cond) ~ temp * state + origin, family = "Gamma",
      data = lake, spcov_type = "cauchy", partition_factor = ~year)
```

Deviance Residuals:

Min	1Q	Median	3Q	Max
-1.35762	-0.20796	-0.03706	0.17869	1.10616

Coefficients (fixed):

Estimate	Std. Error	z value	Pr(> z)
----------	------------	---------	----------

```
(Intercept) 3.59325 0.50058 7.178 7.06e-13 ***
temp 0.15182 0.03006 5.051 4.39e-07 ***
stateCO -0.03214 0.56098 -0.057 0.95432
stateNV 0.75664 0.66851 1.132 0.25771
stateUT -0.19696 0.55916 -0.352 0.72466
originNATURAL 0.08313 0.21988 0.378 0.70538
temp:stateCO 0.13679 0.04808 2.845 0.00444 **
temp:stateNV 0.01882 0.05820 0.323 0.74645
temp:stateUT 0.20015 0.04846 4.131 3.62e-05 ***
---
Signif. codes: 0 '***' 0.001 '**' 0.01 '*' 0.05 '.' 0.1 ' ' 1

Pseudo R-squared: 0.7061

Coefficients (cauchy spatial covariance):
de ie range extra
2.069e-02 2.952e-01 4.119e+06 5.645e-01

Coefficients (Dispersion for Gamma family):
dispersion
3.761
```

- ⁴⁴¹ A more effective approach is to use an analysis of variance (ANOVA), which is well-suited to
⁴⁴² assess the overall significance of each variable:

```
R> anova(spgam)

Analysis of Variance Table

Response: exp(log_cond)
          Df  Chi2 Pr(>Chi2)
(Intercept) 1 51.5270 7.062e-13 ***
temp         1 25.5146 4.390e-07 ***
state        3  3.0747 0.3802528
origin       1  0.1429 0.7053819
temp:state   3 19.7668 0.0001897 ***
---
Signif. codes: 0 '***' 0.001 '**' 0.01 '*' 0.05 '.' 0.1 ' ' 1
```

- ⁴⁴³ The main effect for temperature and the temperature by state interaction are highly significant
⁴⁴⁴ (p -value < 0.001), while the main effects for state and lake origin are not significant.
⁴⁴⁵ Variance inflation factors assess the degree to which standard errors $\hat{\beta}$ are inflated due to
⁴⁴⁶ covariance among the columns of \mathbf{X} . Generalized variance inflation factors can capture the
⁴⁴⁷ variance inflation for subsets of \mathbf{X} that may include categorical variables with more than two
⁴⁴⁸ levels (Fox and Monette 1992):

```
R> library(car)
```

```
R> vif(spgam)
```

	GVIF	Df	GVIF^(1/(2*Df))
temp	4.691914	1	2.166083
state	127.082397	3	2.242234
origin	1.264940	1	1.124695
temp:state	76.387383	3	2.059856

- 449 The GVIF^{1/2df} values for `temp`, `state`, and `temp:state` are just greater than two, which
 450 suggests moderate multicollinearity for these terms – unsurprising given the `temp:state`
 451 interaction in the model. The GVIF^{1/2df} for `origin` is close to one, which suggests little to
 452 no multicollinearity for this term.
- 453 Because of the interaction between `temp` and `state`, contrasts that assess mean differences
 454 among states should condition upon a specific temperature value. By default, `emmeans` uses
 455 the mean temperature value (here, 7.63) to assess contrasts:

```
R> library(emmeans)
```

```
R> pairs(emmeans(spgam, ~ state | temp))
```

temp = 7.63:					
contrast	estimate	SE	df	z.ratio	p.value
AZ - CO	-1.012	0.337	Inf	-3.004	0.0142
AZ - NV	-0.900	0.348	Inf	-2.584	0.0480
AZ - UT	-1.331	0.326	Inf	-4.082	0.0003
CO - NV	0.112	0.258	Inf	0.434	0.9727
CO - UT	-0.319	0.223	Inf	-1.427	0.4822
NV - UT	-0.431	0.244	Inf	-1.763	0.2915

```
Results are averaged over the levels of: origin
Degrees-of-freedom method: asymptotic
Results are given on the log (not the response) scale.
P value adjustment: tukey method for comparing a family of 4 estimates
```

- 456 Again, because of the interaction between `temp` and `state`, we should assess temperature
 457 trends separately for each state:

```
R> emtrends(spgam, ~ state, var = "temp")
```

state	temp.trend	SE	df	asymp.LCL	asymp.UCL
AZ	0.152	0.0301	Inf	0.0929	0.211
CO	0.289	0.0370	Inf	0.2161	0.361
NV	0.171	0.0504	Inf	0.0718	0.270
UT	0.352	0.0372	Inf	0.2791	0.425

```
Results are averaged over the levels of: origin
```

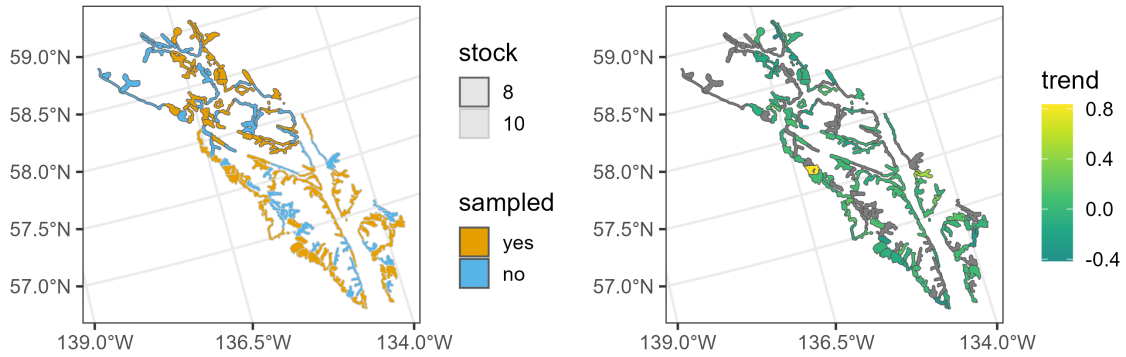


Figure 10: Seal trend distribution in Alaska. Observed and missing seal polygons by stock (left) and observed log seal trends (right).

```
Degrees-of-freedom method: asymptotic
Results are given on the exp (not the response) scale.
Confidence level used: 0.95
```

458 4.3. Modeling harbor seal trends in Alaska, USA

459 The **seal** data in **spmodel** contains harbor seal abundance trends for two different harbor
 460 stocks (genetically distinct populations). While the **moose** and **lake** data were point-
 461 referenced, the **seal** data are areal. Each polygon in the **seal** data represents a distinct
 462 harbor seal haulout region (Figure 10). A haulout region is an area of coastal rocks that
 463 harbor seals go to rest, molt, and give birth.

464 For each polygon, a Poisson regression was used to quantify the mean trend in abundance
 465 over approximately 30 years (Ver Hoef, Peterson, Hooten, Hanks, and Fortin 2018). If the
 466 logarithm of mean abundance trends (`log_trend`) is negative (positive), it means abundance
 467 is decreasing (increasing). We use a binomial SPGLM to quantify the likelihood that mean
 468 abundance trends are decreasing:

```
R> is_decreasing <- seal$log_trend < 0
R> spbin <- spgautor(
+   formula = is_decreasing ~ 1,
+   family = binomial,
+   data = seal,
+   spcov_type = "car",
+   random = ~ stock
+ )
```

469 To model spatial dependence, we used a conditional autoregressive function. Conditional
 470 and simultaneous autoregressive functions characterize spatial distance through neighborhood
 471 relationships (rather than Euclidean distance) and have `spcov_type` values of "car" and
 472 "sar", respectively. By default, Queen's distance is used to determine whether two sites are
 473 neighbors, though custom neighborhood matrices can be passed via `W`. Row standardization

474 is also assumed by default; this can be changed via `row_st`. Using `random`, we also specified
 475 a nonspatial random effect for seal stock. The `random` argument uses similar syntax as `lme4`
 476 (Bates, Mächler, Bolker, and Walker 2015) and `nlme` (Pinheiro and Bates 2006) to specify
 477 nonspatial random effects.

478 Tidying the model reveals the estimates and confidence intervals on the log odds scale:

```
R> tidy(spbin, conf.int = TRUE)
```

```
# A tibble: 1 x 7
  term      estimate std.error statistic p.value conf.low conf.high
  <chr>     <dbl>     <dbl>     <dbl>    <dbl>    <dbl>    <dbl>
1 (Intercept) 0.340     0.673     0.506   0.613   -0.979    1.66
```

479 Back-transforming the confidence interval to the probability scale yields:

```
R> emmeans(spbin, ~ 1, type = "response")
```

```
1      prob      SE  df asymp.LCL asymp.UCL
overall 0.584 0.164 Inf      0.273      0.84
```

```
Degrees-of-freedom method: asymptotic
Confidence level used: 0.95
Intervals are back-transformed from the logit scale
```

480 The `SE` column is the standard error on the response scale obtained from the delta method
 481 (Oehlert 1992).

482 In contrast to point-referenced data, prediction locations for areal data must be specified
 483 at the time of model fitting, as they affect the spatial covariance function's neighborhood
 484 structure. Prediction locations whose response values have an `NA` (i.e., missing) value are
 485 converted into a `newdata` object that is stored in the model output. For example, rows one
 486 and nine are locations without seal trends, meaning they are not used in model fitting but
 487 are desired for prediction:

```
R> seal
```

```
Simple feature collection with 149 features and 2 fields
Geometry type: POLYGON
Dimension:      XY
Bounding box:  xmin: 913618.8 ymin: 855730.2 xmax: 1221859 ymax: 1145054
Projected CRS: NAD83 / Alaska Albers
# A tibble: 149 x 3
  log_trend stock                               geometry
  *      <dbl> <fct>                           <POLYGON [m]>
1    NA      8      ((1035002 1054710, 1035002 1054542, 1035002 105354~
2   -0.282    8      ((1037002 1039492, 1037006 1039490, 1037017 103949~
3  -0.00121   8      ((1070158 1030216, 1070185 1030207, 1070187 103020~
```

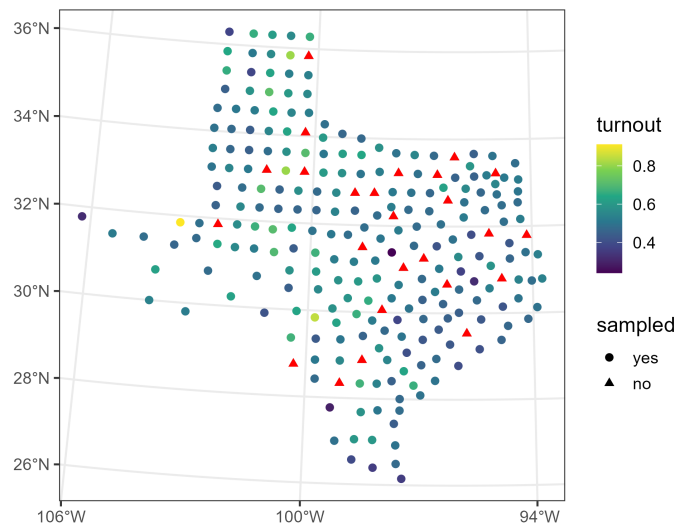


Figure 11: Proportion of voter turnout in Texas for the 1980 presidential election. Circles represent voter turnout (based on color) and triangles represent locations at which voter turnout predictions are desired.

```

4   0.0354  8    ((1054906 1034826, 1054931 1034821, 1054936 103482~
5  -0.0160  8    ((1025142 1056940, 1025184 1056889, 1025222 105683~
6   0.0872  8    ((1026035 1044623, 1026037 1044605, 1026072 104461~
7  -0.266   8    ((1100345 1060709, 1100287 1060706, 1100228 106070~
8   0.0743  8    ((1030247 1029637, 1030248 1029637, 1030265 102964~
9   NA      8    ((1043093 1020553, 1043097 1020550, 1043101 102055~
10  -0.00961 8    ((1116002 1024542, 1116002 1023542, 1116002 102254~
# i 139 more rows

```

⁴⁸⁸ Then, `predict()` can be called without having to specify `newdata`:

```
R> predict(spin, type = "response", interval = "prediction")[1:5, ]
```

	fit	lwr	upr
1	0.6807677	0.3863736	0.8783808
9	0.5945680	0.2467634	0.8678078
13	0.6189055	0.2974432	0.8616799
15	0.6040102	0.2921802	0.8493132
18	0.6375700	0.3356282	0.8596641

⁴⁸⁹ We could have alternatively used a (geostatistical) SPGLM via `spglm()`. When areal data are
⁴⁹⁰ used with `spglm()`, the centroids of each polygon are used as the point-referenced coordinates.
⁴⁹¹ We further explore comparisons between point-referenced and aerial data in the next example.

⁴⁹² 4.4. Modeling voter turnout in Texas, USA

493 The **texas** data in **spmodel** contains voter turnout data for Texas counties in the 1980 United
 494 States Presidential Election (Bivand, Nowosad, and Lovelace 2024). The data are point-
 495 referenced, with polygon centroids representing the spatial location of each county (Figure 11).
 496 Beta regression is a GLM used to model rate and proportion data in the (0, 1) interval (Ferrari
 497 and Cribari-Neto 2004; Cribari-Neto and Zeileis 2010). We model voter turnout rates as a
 498 function of mean log income of county residents using an SPGLM assuming a beta distributed
 499 response variable:

```
R> spbeta_geo <- spglm(
+   formula = turnout ~ log_income,
+   family = "beta",
+   data = texas,
+   spcov_type = "matern"
+ )
```

500 Alternatively, we could use an autoregressive model to fit the model, constructing a neighbor-
 501 hood matrix by assuming centroids within **cutoff** of one another are neighbors:

```
R> spbeta_auto <- spgautor(
+   formula = turnout ~ log_income,
+   family = "beta",
+   data = texas,
+   spcov_type = "car",
+   cutoff = 1e5
+ )
```

502 According to AIC, the SPGLM for point-referenced data is preferred:

```
R> AIC(spbeta_geo, spbeta_auto)
```

	df	AIC
spbeta_geo	5	-44.53113
spbeta_auto	3	-22.46104

503 The default estimation method in **spmodel** for SPGLMs is restricted maximum likelihood
 504 (REML), while maximum likelihood (ML) can also be used. A benefit of REML
 505 is that it can yield unbiased estimates of covariance parameters (Cressie and Lahiri 1993),
 506 but a drawback is that likelihood-based statistics are only valid for model comparison when
 507 the models have the same explanatory variable and fixed effect structure (because the error
 508 contrasts used to construct the REML likelihood change based on \mathbf{X} and $\boldsymbol{\beta}$). In contrast,
 509 ML estimators are biased, though in practice this bias may be small. Moreover, when using
 510 ML, likelihood-based comparisons are valid for models having different explanatory variable
 511 and fixed effect structures. Using ML, we can evaluate the significance of log income on voter
 512 turnout with a likelihood ratio test:

```
R> spbeta_full_ml <- update(spbeta_geo, estmethod = "ml")
R> spbeta_red_ml <- update(spbeta_geo, estmethod = "ml", formula = turnout ~ 1)
R> anova(spbeta_full_ml, spbeta_red_ml)
```

Likelihood Ratio Test

```
Response: turnout
          Df    Chi2 Pr(>Chi2)
spbeta_red_ml vs spbeta_full_ml 1 23.155 1.494e-06 ***
---
Signif. codes: 0 '***' 0.001 '**' 0.01 '*' 0.05 '.' 0.1 ' ' 1
```

513 The likelihood ratio test suggests that log income is significantly related to voter turnout (p -
 514 value < 0.001). Alternatively, we could have instead used a different likelihood-based statistic
 515 like AIC:

```
R> AIC(spbeta_full_ml, spbeta_red_ml)
```

	df	AIC
spbeta_full_ml	7	-31.25900
spbeta_red_ml	6	-10.10354

516 The AIC also prefers the full model, suggesting that log income is important for predicting
 517 voter turnout.

5. Discussion

518 SPGLMs are fit in **spmodel** using a novel application of the Laplace approximation that
 519 simultaneously marginalizes over the latent (i.e., unobserved) random effects and the fixed
 520 effects, β . The approach is very flexible and accommodates general response distributions and
 521 covariance structures, though here we focus on spatial applications. **spmodel**'s **spglm()** and
 522 **spgautor()** fit SPGLMs that are similar in structure and syntax as base R's **glm()** function,
 523 easing the transition from GLMs to SPGLMs for practitioners. The **spglm()** and **spgautor()**
 524 functions support six response distributions for binary, count, and skewed data and 20 spatial
 525 covariance functions. **spmodel** also provides a suite of tools for data visualization, inference,
 526 model diagnostics, and prediction, providing a framework that can be used for all stages of a
 527 data analysis. There are many additional **spmodel** features that are not covered here, includ-
 528 ing fitting multiple models simultaneously, fixing spatial covariance and dispersion parameters
 529 at known values, fitting models to large non-Gaussian data having thousands of observations
 530 via spatial indexing (Ver Hoef, Dumelle, Higham, Peterson, and Isaak 2023), incorporating
 531 spatial dependence in machine learning (e.g., random forests; Breiman (2001)), simulating
 532 spatially dependent data (e.g., **spbinom()**, **sprpois()**, etc.), and more. Further details are
 533 provided by <https://CRAN.R-project.org/package=spmodel> and links therein.

Computational details

534 The results in this paper were obtained using R 4.4.0 with the **spmodel** 0.11.0 package. Figures
 535 were created using the **ggplot2** 3.5.1 package (Wickham 2016) and base R.

Data and code availability

536 All writing and code associated with this manuscript is available for viewing and download on
 537 GitHub at <https://github.com/USEPA/spmodel.glm.manuscript>. All data used are part
 538 of the **spmodel** R package available for download from CRAN at <https://CRAN.R-project.org/package=spmodel>.
 539

Acknowledgments

540 We would like to thank initial reviewers and editors for feedback that has greatly improved
 541 the manuscript.
 542 The views expressed in this manuscript are those of the authors and do not necessarily
 543 represent the views or policies of the U.S. Environmental Protection Agency or the National
 544 Oceanic and Atmospheric Administration. Any mention of trade names, products, or services
 545 does not imply an endorsement by the U.S. government, the U.S. Environmental Protection
 546 Agency, or the National Oceanic and Atmospheric Administration. The U.S. Environmental
 547 Protection Agency and the National Oceanic and Atmospheric Administration do not endorse
 548 any commercial products, services or enterprises.

References

- 549 Akaike H (1974). “A New Look at the Statistical Model Identification.” *IEEE Transactions*
 550 *on Automatic Control*, **19**(6), 716–723.
- 551 Anderson SC, Ward EJ, English PA, Barnett LAK, Thorson JT (2024). “sdmTMB: an R
 552 package for fast, flexible, and user-friendly generalized linear mixed effects models with
 553 spatial and spatiotemporal random fields.” *bioRxiv*, **2022.03.24.485545**. doi:[10.1101/2022.03.24.485545](https://doi.org/10.1101/2022.03.24.485545).
- 555 Bachl FE, Lindgren F, Borchers DL, Illian JB (2019). “inlabru: an R package for Bayesian
 556 spatial modelling from ecological survey data.” *Methods in Ecology and Evolution*, **10**,
 557 760–766. doi:[10.1111/2041-210X.13168](https://doi.org/10.1111/2041-210X.13168).
- 558 Bates D, Mächler M, Bolker B, Walker S (2015). “Fitting Linear Mixed-Effects Models Using
 559 lme4.” *Journal of Statistical Software*, **67**(1), 1–48. doi:[10.18637/jss.v067.i01](https://doi.org/10.18637/jss.v067.i01).
- 560 Bivand R, Nowosad J, Lovelace R (2024). *spData: Datasets for Spatial Analysis*. R package
 561 version 2.3.1, URL <https://CRAN.R-project.org/package=spData>.
- 562 Bolker BM, Brooks ME, Clark CJ, Geange SW, Poulsen JR, Stevens MHH, White JSS (2009).
 563 “Generalized Linear Mixed Models: A Practical Guide for Ecology and Evolution.” *Trends*
 564 *in Ecology & Evolution*, **24**(3), 127–135.
- 565 Bonat WH, Ribeiro Jr PJ (2016). “Practical likelihood analysis for spatial generalized linear
 566 mixed models.” *Environmetrics*, **27**(2), 83–89.
- 567 Breiman L (2001). “Random forests.” *Machine Learning*, **45**, 5–32.

- 568 Breslow NE, Clayton DG (1993). “Approximate Inference in Generalized Linear Mixed Mod-
569 els.” *Journal of the American Statistical Association*, **88**(421), 9–25.
- 570 Brooks ME, Kristensen K, van Benthem KJ, Magnusson A, Berg CW, Nielsen A, Skaug
571 HJ, Maechler M, Bolker BM (2017). “glmmTMB Balances Speed and Flexibility Among
572 Packages for Zero-Inflated Generalized Linear Mixed Modeling.” *The R Journal*, **9**(2),
573 378–400. [doi:10.32614/RJ-2017-066](https://doi.org/10.32614/RJ-2017-066).
- 574 Bürkner PC (2017). “brms: An R package for Bayesian Multilevel Models Using Stan.”
575 *Journal of Statistical Software*, **80**, 1–28.
- 576 Chambers JM, Hastie TJ (eds.) (1992). *Statistical Models in S*. Chapman & Hall, London.
- 577 Cook RD (1979). “Influential Observations in Linear Regression.” *Journal of the American
578 Statistical Association*, **74**(365), 169–174.
- 579 Cook RD, Weisberg S (1982). *Residuals and Influence in Regression*. New York: Chapman
580 and Hall.
- 581 Cressie N (1990). “The origins of kriging.” *Mathematical geology*, **22**(3), 239–252.
- 582 Cressie N (1993). *Statistics for Spatial Data*. John Wiley & Sons.
- 583 Cressie N, Lahiri SN (1993). “The asymptotic distribution of REML estimators.” *Journal of
584 multivariate analysis*, **45**(2), 217–233.
- 585 Cribari-Neto F, Zeileis A (2010). “Beta regression in R.” *Journal of statistical software*, **34**(1),
586 1–24.
- 587 Doser JW, Finley AO, Kéry M, Zipkin EF (2022). “spOccupancy: An R package for single-
588 species, multi-species, and integrated spatial occupancy models.” *Methods in Ecology and
589 Evolution*, **13**(8), 1670–1678.
- 590 Doser JW, Finley AO, Kéry M, Zipkin EF (2024). “spAbundance: An R package for single-
591 species and multi-species spatially explicit abundance models.” *Methods in Ecology and
592 Evolution*, **15**(6), 1024–1033.
- 593 Dumelle M, Higham M, Ver Hoef JM (2023). “spmodel: Spatial Statistical Modeling and
594 Prediction in R.” *PLOS ONE*, **18**(3), e0282524.
- 595 Evangelou E, Zhu Z, Smith RL (2011). “Estimation and prediction for spatial generalized lin-
596 ear mixed models using high order Laplace approximation.” *Journal of Statistical Planning
597 and Inference*, **141**(11), 3564–3577.
- 598 Faraway JJ (2016). *Extending the Linear Model with R: Generalized Linear, Mixed Effects
599 and Nonparametric Regression Models*. CRC press.
- 600 Ferrari S, Cribari-Neto F (2004). “Beta Regression for Modelling Rates and Proportions.”
601 *Journal of applied statistics*, **31**(7), 799–815.
- 602 Finley AO, Banerjee S, Carlin BP (2007). “spBayes: An R Package for Univariate and
603 Multivariate Hierarchical Point-Referenced Spatial Models.” *Journal of Statistical Software*,
604 **19**(4), 1–24. URL <https://www.jstatsoft.org/article/view/v019i04>.

- 605 Finley AO, Datta A, Banerjee S (2022). “spNNGP R Package for Nearest Neighbor Gaussian
 606 Process Models.” *Journal of Statistical Software*, **103**(5), 1–40. [doi:10.18637/jss.v103.i05](https://doi.org/10.18637/jss.v103.i05).
- 608 Fox J, Monette G (1992). “Generalized collinearity diagnostics.” *Journal of the American
 609 Statistical Association*, **87**(417), 178–183.
- 610 Fox J, Weisberg S (2019). *An R Companion to Applied Regression*. Third edition. Sage,
 611 Thousand Oaks CA. URL <https://www.john-fox.ca/Companion/>.
- 612 Harville DA (1977). “Maximum Likelihood Approaches to Variance Component Estimation
 613 and to Related Problems.” *Journal of the American Statistical Association*, **72**(358), 320–
 614 338.
- 615 Hoeting JA, Davis RA, Merton AA, Thompson SE (2006). “Model Selection for Geostatistical
 616 Models.” *Ecological Applications*, **16**(1), 87–98.
- 617 Hughes J, Cui X (2020). *ngspatial: Fitting the Centered Autologistic and Sparse Spatial
 618 Generalized Linear Mixed Models for Areal Data*. Frederick, MD. R package version 1.2-2.
- 619 James G, Witten D, Hastie T, Tibshirani R (2013). *An Introduction to Statistical Learning*.
 620 Springer-Verlag.
- 621 Kuhn M, Silge J (2022). *Tidy Modeling with R*. O'Reilly Media, Inc.
- 622 Lee D (2013). “CARBayes: An R Package for Bayesian Spatial Modeling with Conditional
 623 Autoregressive Priors.” *Journal of Statistical Software*, **55**(13), 1–24.
- 624 Lee Y, Nelder JA (1996). “Hierarchical Generalized Linear Models.” *Journal of the Royal
 625 Statistical Society: Series B (Methodological)*, **58**(4), 619–656.
- 626 Lenth RV (2024). *emmeans: Estimated Marginal Means, aka Least-Squares Means*. R package
 627 version 1.10.3, URL <https://CRAN.R-project.org/package=emmeans>.
- 628 Lindgren F, Rue H (2015). “Bayesian Spatial Modelling with R-INLA.” *Journal of Statistical
 629 Software*, **63**, 1–25.
- 630 McCullagh P, Nelder JA (1989). *Generalized Linear Models, Second Edition*. Chapman and
 631 Hall Ltd.
- 632 Montgomery DC, Peck EA, Vining GG (2021). *Introduction to Linear Regression Analysis*.
 633 John Wiley & Sons.
- 634 Myers RH, Montgomery DC, Vining GG, Robinson TJ (2012). *Generalized Linear Models:
 635 With Applications in Engineering and the Sciences*. John Wiley & Sons.
- 636 Nelder JA, Wedderburn RW (1972). “Generalized Linear Models.” *Journal of the Royal
 637 Statistical Society: Series A (General)*, **135**(3), 370–384.
- 638 Oehlert GW (1992). “A note on the delta method.” *The American Statistician*, **46**(1), 27–29.
- 639 Patterson D, Thompson R (1971). “Recovery of Inter-Block Information when Block Sizes
 640 are Unequal.” *Biometrika*, **58**(3), 545–554.

- 641 Pebesma E (2018). “Simple Features for R: Standardized Support for Spatial Vector Data.”
642 *The R Journal*, **10**(1), 439–446. doi:10.32614/RJ-2018-009. URL <https://doi.org/10.32614/RJ-2018-009>.
- 644 Pinheiro J, Bates D (2006). *Mixed-Effects Models in S and S-PLUS*. Springer-Verlag Science
645 & Business Media.
- 646 R Core Team (2024). *R: A Language and Environment for Statistical Computing*. R Foun-
647 dation for Statistical Computing, Vienna, Austria. URL <https://www.R-project.org/>.
- 648 Rencher AC, Schaalje GB (2008). *Linear models in statistics*. John Wiley & Sons.
- 649 Robinson D, Hayes A, Couch S (2021). *broom: Convert Statistical Objects into Tidy Tibbles*.
650 R package version 0.7.6, URL <https://CRAN.R-project.org/package=broom>.
- 651 Ronnegard L, Shen X, Alam M (2010). “hglm: A Package for Fitting Hierarchical Generalized
652 Linear Models.” *The R Journal*, **2**(2), 20–28.
- 653 Rousset F, Ferdy JB (2014). “Testing Environmental and Genetic Effects in the Presence
654 of Spatial Autocorrelation.” *Ecography*, **37**(8), 781–790. URL <https://dx.doi.org/10.1111/ecog.00566>.
- 655 Sainsbury-Dale M, Zammit-Mangion A, Cressie N (2024). “Modeling Big, Heterogeneous,
656 Non-Gaussian Spatial and Spatio-Temporal Data Using FRK.” *Journal of Statistical Soft-
657 ware*, **108**, 1–39.
- 659 Schwarz G (1978). “Estimating the Dimension of a Model.” *The Annals of Statistics*, pp.
660 461–464.
- 661 Smith TJ, McKenna CM (2013). “A comparison of logistic regression pseudo R2 indices.”
662 *General Linear Model Journal*, **39**(2), 17–26.
- 663 Stein ML (1999). *Interpolation of spatial data: Some theory for Kriging*. Springer-Verlag
664 Science & Business Media.
- 665 Thorson JT, Anderson SC, Goddard P, Rooper CN (2025). “tinyVAST: R package with
666 an expressive interface to specify lagged and simultaneous effects in multivariate spatio-
667 temporal models.” *Global Ecology and Biogeography*, **34**(4), e70035. doi:10.1111/geb.
668 70035. URL <https://doi.org/10.1111/geb.70035>.
- 669 Tobler WR (1970). “A Computer Movie Simulating Urban Growth in the Detroit Region.”
670 *Economic Geography*, **46**(sup1), 234–240.
- 671 Tredennick AT, Hooker G, Ellner SP, Adler PB (2021). “A practical guide to selecting models
672 for exploration, inference, and prediction in ecology.” *Ecology*, **102**(6), e03336.
- 673 Ver Hoef JM, Blagg E, Dumelle M, Dixon PM, Zimmerman DL, Conn PB (2024). “Marginal
674 Inference for Hierarchical Generalized Linear Mixed Models with Patterned Covariance
675 Matrices Using the Laplace Approximation.” *Environmetrics*, **35**(7), e2872. doi:10.1002/
676 env.2872.
- 677 Ver Hoef JM, Dumelle M, Higham M, Peterson EE, Isaak DJ (2023). “Indexing and Parti-
678 tioning the Spatial Linear Model for Large Data Sets.” *PLOS ONE*, **18**(11), e0291906.

- 679 Ver Hoef JM, Peterson EE, Hooten MB, Hanks EM, Fortin MJ (2018). “Spatial Autoregressive
 680 Models for Statistical Inference From Ecological Data.” *Ecological Monographs*, **88**(1), 36–
 681 59.
- 682 Wedderburn RW (1974). “Quasi-Likelihood Functions, Generalized Linear Models, and the
 683 Gauss—Newton Method.” *Biometrika*, **61**(3), 439–447.
- 684 Wickham H (2016). *ggplot2: Elegant Graphics for Data Analysis*. Springer-Verlag, New York.
 685 ISBN 978-3-319-24277-4. URL <https://ggplot2.tidyverse.org>.
- 686 Wolfinger R, O’connell M (1993). “Generalized Linear Mixed Models: A Pseudo-Likelihood
 687 Approach.” *Journal of Statistical Computation and Simulation*, **48**(3-4), 233–243.
- 688 Wolfinger R, Tobias R, Sall J (1994). “Computing Gaussian Likelihoods and their Derivatives
 689 for General Linear Mixed Models.” *SIAM Journal on Scientific Computing*, **15**(6), 1294–
 690 1310.
- 691 Wood SN (2017). *Generalized Additive Models: An Introduction with R*. CRC press.
- 692 Zimmerman DL, Ver Hoef JM (2024). *Spatial Linear Models for Environmental Data*. CRC
 693 Press.

694 **Affiliation:**

695 Michael Dumelle
 696 United States
 697 Environmental Protection Agency
 698 200 SW 35th St
 699 Corvallis, OR, 97330
 700 E-mail: Dumelle.Michael@epa.gov
 701